

1198
C.1

ENGINEERING DEPT. LIBRARY
CHANCE VOUGHT AIRCRAFT
STRATFORD, CONN.

NATIONAL ADVISORY COMMITTEE FOR AERONAUTICS

TECHNICAL NOTE

No. 1198

SOME INVESTIGATIONS OF THE GENERAL INSTABILITY
OF STIFFENED METAL CYLINDERS

IX - CRITERIONS FOR THE DESIGN OF STIFFENED
METAL CYLINDERS SUBJECT TO GENERAL
INSTABILITY FAILURES

By Louis G. Dunn

California Institute of Technology



Washington
November 1947

NATIONAL ADVISORY COMMITTEE FOR AERONAUTICS

TECHNICAL NOTE NO. 1198

SOME INVESTIGATIONS OF THE GENERAL INSTABILITY OF STIFFENED METAL CYLINDERS

IX - CRITERIONS FOR THE DESIGN OF STIFFENED METAL CYLINDERS SUBJECT

TO GENERAL INSTABILITY FAILURES

By Louis G. Dunn

SUMMARY

An experimental investigation of the general instability of reinforced thin-walled metal cylinders was made at the California Institute of Technology, and a summary of the pertinent design information that was gathered during the course of the investigation is given in the present report. As a result of this investigation, parameters were evolved which make it possible to obtain an estimate of the stress at which general instability will occur for any given stiffened metal structure of circular cross section. It is considered that both the geometrical quantities and sectional properties of the structural members were varied over a sufficient range to establish, in general, the validity of the parameters. Because of the catastrophic nature of a general instability failure it is recommended that ample margins of safety be allowed in an airplane structure in which this type of failure might occur.

A theoretical treatment of the general-instability problem was not given because of the nonlinearity of the buckling problem of stiffened cylinders. The parameters presented for predicting the ultimate strength of stiffened metal cylinders subjected to pure bending and pure torsion were based on an analysis of the experimental results and on the existing theory of unstiffened metal cylinders. This method was preferred to that of a linearized theory which cannot correctly describe the behavior of the structure. The results of a linear theory would have to be modified and corrected to bring it into agreement with the experimental observations, and thus the theory would immediately be rendered an empirical method.

INTRODUCTION

With the extensive use of thin metal sheet in aircraft fabrication a number of new design problems were introduced. Of these problems, a large number have either been solved or sufficient knowledge regarding them exists to enable the engineer to design satisfactory airplane structures. However, with the rapidly increasing size of modern airplanes, a number of new structural problems arise, one of these being the problem of determining the allowable loads that can be carried by stiffened cylinders of large radius. It is known that certain combinations of longitudinal stiffeners, frames, and sheet will give a cylinder that will fail in such a manner as to involve all three structural elements simultaneously. This type of failure is referred to as the general instability failure of a stiffened cylinder. The parameters affecting the failing load of such a structure are of primary importance in the design of large airplanes.

In view of the fact that acceptable methods were not available for the design of large stiffened cylinders, the Civil Aeronautics Authority started the sponsorship of a research program at the California Institute of Technology. The investigation covering the failure of stiffened cylinders subjected to pure bending was carried out under this sponsorship. The investigation of stiffened cylinders subjected to combined loadings and to pure torsion was carried out under the sponsorship and with the financial assistance of the National Advisory Committee for Aeronautics.

In general, the purpose of the investigation was to determine two things:

- (a) A method of calculating the strength of cylindrical structures falling into the general-instability classification
- (b) The limits of the general-instability regime

The results of the investigation have been presented in detail in references 1 to 8, and the present report summarizes the pertinent design information gathered during the course of the investigation.

ANALYSIS OF PROBLEM AND BASIS OF THEORY

In order to clarify the meaning of general instability and why it may be considered as being a problem peculiar to large airplanes, the functions which the elements of a stiffened metal cylinder must perform and the types of failure which may occur should be considered briefly.

Stiffened shells as used in metal aircraft construction consist primarily of the following elements:

- (a) The sheet-metal covering
- (b) The longitudinal stiffening elements
- (c) The transverse stiffening elements, generally referred to as ribs, bulkheads, or frames

The functions of the sheet-metal covering are to provide an aerodynamical surface upon which the air forces act (wings and control surfaces) and to furnish a covering for the contents of the airplane. In addition to these functions, the sheet covering is so designed that it is a load-resisting element and as such can be considered as part of the primary structure. In general, part of the load acting on an airplane structure will be compressive in nature. Since thin sheet is weak in compression, it is necessary to provide stiffening elements which will fulfill one or both of two requirements; namely:

- (a) Add additional strength in resisting compressive loads.
- (b) Maintain the aerodynamic shape of the airplane.

In a fuselage, for example, the first is accomplished by attaching stiffening members to the sheet parallel to the axis of the cylinder; and the second, by placing members of the proper shape perpendicular to the cylinder axis. These perpendicular members also act as supports for the longitudinal members. In the following discussion the terms "longitudinal" and "frame" will be used to denote these two classes of members, respectively.

If a cylindrical structure of this type is subjected to compressive loads parallel to its axis, it may fail in one of four distinct ways. The types of failure may be conveniently classified as material failure, local instability, panel instability, and general instability.

In general, the bending-stress distribution is, for purposes of analysis, assumed to be in accord with the elementary beam theory. When buckling of the sheet occurs, appropriate modifications are made in calculating section properties to allow for the reduction in the load-carrying ability of the buckled sheet. The first type of failure therefore offers no difficulty to the designer, since it is necessary that only the ultimate strength of the material be known in order to determine the strength of the structure as a whole.

Local instability generally occurs in sections having wide and thin flanges and is characterized by an instability failure of some small

portion of either a frame or longitudinal. This collapse of part of the stiffening member will precipitate its failure as a column and may also cause premature failure of the whole surrounding structure. The length of the portion of the member involved in local buckling is of the same order of magnitude as its cross-sectional dimensions, and the local buckling stress is not, in general, a function of the total length of the member. The buckling stress of such sections can be either calculated or determined experimentally.

A panel instability failure is defined as one which will occur over a length of structure equal to one frame spacing and which is not caused by local instability spreading to adjacent members. This type of failure will occur in a structure having relatively heavy frames and light longitudinals, the structure tending to act as a number of isolated, axially stiffened cylinders, each of which is one frame spacing in length. Failure will occur by some form of instability of the longitudinals, the magnitude of the failure load being dependent upon the column or torsional strength of the longitudinals, modified by the effect of the attached buckled sheet. The only function of the frames in this case will be to determine the end fixity coefficient of the longitudinals. In the past, the design of stiffened shell structures has been based almost entirely on failures of the panel type. Although an accurate theoretical treatment of the strength properties of curved stiffened panels is not yet available, it has been possible by experimental methods to design structures in which failures tended to fall in the panel-instability classification.

The general-instability type of failure will occur in a structure which has frames and longitudinals of such a size that both will fail simultaneously under the critical load, that is, collapse takes place in such a manner as to destroy the load-carrying properties of all three structural elements - sheet, frames, and longitudinals. The first three types of failure may occur regardless of the size of the airplane. In smaller airplanes (gross weight of 25,000 lb or less) the frame sizes are determined by considerations of local loading conditions and practical manufacturing demands, rather than by requirements for stability. These considerations lead to frames which are sufficiently rigid to preclude the possibility of general instability failures. As airplane sizes increase, these considerations do not require a proportionate increase in frame sizes; consequently, the relative dimensions of the three structural elements may be very small compared with the external dimensions of the structure. Since general instability is a function of the stiffness of the structure as a whole, its occurrence in large airplanes is quite possible and should be investigated.

Although a complete and exact theoretical treatment of the general instability of stiffened cylinders is probably unattainable, the validity of the results obtained from a theoretical treatment of the problem will

depend upon how closely the basic assumptions resemble the actual physical conditions. It is therefore desirable to consider the basic assumptions underlying these treatments.

Of the two possible types of failure which fall into the class of general instability, one occurs under bending loads and is characterized by a general flattening of the cylinder. This type of failure was discussed by L. G. Brazier, for the case of the unstiffened shell under pure bending, and his results have been applied to the stiffened shell problem by N. J. Hoff (reference 9). Both theory and experiment indicate that for general flattening to occur, the length-diameter ratio of the cylinder must be so large that it is completely out of the range of aircraft structures.

The second class of failure, for which two theoretical treatments are available, is that in which the wave form of the buckle is multi-lobed in nature and has, in general, a wave length less than the total length of the cylinder. This buckling form corresponds to the usual "diamond-shaped" wave pattern which is observed in the failure of unstiffened cylinders under compressive loads. One method of investigation distributes the stiffnesses of the longitudinals and frames over the entire cylinder, forming an unstiffened orthotropic cylinder, which is treated as a simple unstiffened cylindrical shell. The thickness and stiffness of this shell in the longitudinal direction differs from that in the circumferential direction by amounts depending upon the areas and stiffnesses of the longitudinals and the frames, respectively. This rearranging of the original stiffened cylinder into an equivalent, unstiffened orthotropic cylinder will be called the equivalent-shell method.

A second method that can be used is to consider the sheet, the longitudinals, and frames as components of a statically indeterminate truss system. The longitudinals and frames, each with its proper effective width of sheet acting, form the normal load-resisting members, while a suitable amount of sheet in each panel acts as a tension diagonal to transmit the shear forces. This method will be called the equivalent-truss method.

Theoretical treatments of this problem have been given in references 9 to 12. In references 10 and 11, the equivalent-shell method has been used, while in reference 9 only the longitudinals and not the stiffness of the frames are distributed, the frames being used as local elastic supports for the longitudinal elements of the shell. The results of the pure-bending tests of reference 5 were later utilized by Hoff in reference 12 to modify his original theory given in reference 9.

With the exception of one test (see reference 9) no experimental data were available on the general instability failure. A systematic

experimental investigation appeared to be necessary to check the validity of the theoretical results and, if no agreement could be obtained with these results, to determine a method of estimating the general-instability stress.

Inasmuch as bending is one of the critical loading conditions for airplane structures and also one of the simplest loading conditions to deal with both experimentally and theoretically it was decided to investigate first the failure of stiffened metal cylinders when subjected to a pure bending moment. It was realized that no airplane structure is subjected to bending moments without a certain amount of attendant direct shear. However, it was felt that a study of the pure-bending phenomenon would form a desirable background for the more complicated problem of bending plus shear and for the more general combined loading conditions.

Upon completion of the pure-bending investigation (reference 5), the experimental work was extended to cover the loading conditions of combined bending and transverse shear (reference 6), combined bending and torsion (reference 7), and pure torsion (reference 8).

Since a condition of a pure torsional load seldom arises in the design of fuselage or wing structures, the problem of pure torsion as such might not warrant an investigation; however, under a combined loading of bending plus torsion (reference 7), the ultimate load of the stiffened cylinder is dependent upon the ratio of the shearing stress at failure for combined loading to the shearing stress at failure for pure torsion. Hence, in order to predict the ultimate strength of a stiffened metal cylinder subjected to combined bending and torsion, a knowledge of the ultimate strength of the cylinder when subjected to a pure torsion loading is necessary.

SYMBOLS

M	applied bending moment, inch-pounds
$M_{T_{max}}$	applied torsional moment at failure, inch-pounds
σ_{st}	compressive stress in longitudinals, pounds per square inch
σ_{cr}	compressive stress in longitudinals at failure (when used in conjunction with the sheet covering or an unstiffened cylinder it corresponds to a buckling stress), pounds per square inch
τ	shearing stress in the sheet covering, pounds per square inch

τ_{max}	shearing stress in the sheet covering at failure, pounds per square inch
τ_{cr}	buckling shear stress of the sheet covering, pounds per square inch
E	Young's modulus, pounds per square inch
E'	effective modulus, pounds per square inch
G_E	effective shear modulus, pounds per square inch
t	thickness of sheet covering, inches
A	area enclosed by sheet covering, square inches
R	radius of cylinder, inches
L	length of cylinder, inches
b	spacing of longitudinals, inches
d	spacing of frames, inches
ρ_x	radius of gyration of a longitudinal and effective sheet, inches
ρ_y	radius of gyration of a frame and effective sheet, inches

TEST PROCEDURE

A description of the test articles and test methods has been given in detail in references 1 to 8, and no further discussion will be given here. For convenience, data pertaining to the various tests are given in tables I to IV. Cross-sectional dimensions, areas, and moments of inertia are given for all the stiffening elements in figure 1. Typical curves of the longitudinal strains for the various loading conditions have been included as follows:

- (a) pure bending, figures 2 to 4
- (b) combined bending and transverse shear, figures 5 to 7
- (c) combined bending and torsion, figures 8 to 11
- (d) pure torsion, figure 12

A number of photographs (figs. 13 to 16) showing the various types of failure are also included.

RESULTS AND DISCUSSION

Pure Bending

The results of a simplified theoretical treatment of the problem (references 9 to 11) were checked experimentally (reference 5) and it was found that they do not give results sufficiently accurate for design purposes.

For a systematic experimental investigation it is necessary first to consider the variables involved in the problem of general instability. These variables may be divided into two classes - those dealing with the geometry of the structure and those which involve the sectional properties of the stiffening elements as well as the sheet covering. The geometrical variables are as follows: the longitudinal spacing b , the frame spacing d , the diameter, and length of the cylinder. The second group of variables includes the section properties of the longitudinals and frames, and the thickness of the sheet covering.

By a systematic variation of these variables it is possible to determine experimentally a suitable parameter for predicting the loads at which a stiffened cylindrical shell will fail by general instability. Investigating first the geometrical variables, b and d , it was found that the reciprocal of the maximum compressive strain at failure varied as $\sqrt[4]{bd}$. The next question was in what manner do the radius R and the section parameters ρ_x and ρ_y influence the design parameter. By analogy with the buckling of unstiffened cylinders it was expected that for identical values of b , d , ρ_x , and ρ_y the reciprocal of the critical value of the strain would vary linearly with R . This assumption was checked experimentally and found to be correct; hence, it was concluded that the design parameter has the form

$$\frac{\sqrt[4]{bd} R}{f(\rho_x, \rho_y)}$$

From dimensional reasoning, it follows that the function $f(\rho_x, \rho_y)$ must have the dimensions of the 3/2 power of a length. The simplest assumption for the function which determines the influence of the section parameters, ρ_x and ρ_y , is that it depends only on the geometrical mean value $\sqrt{\rho_x \rho_y}$. Thus the design parameter appears in the form

$$\frac{\sqrt[4]{bd R}}{(\rho_x \rho_y)^{3/4}}$$

or

$$\frac{R}{\sqrt{\rho_x \rho_y}} \sqrt[4]{\frac{bd}{\rho_x \rho_y}}$$

Hence, the maximum strain at failure is given by an equation of the form

$$\frac{\sigma_{cr}}{E'} = \frac{k_1 \sqrt{\rho_x \rho_y}}{R} \sqrt[4]{\frac{\rho_x \rho_y}{bd}} \quad (1)$$

Concerning the width of sheet to be used with the longitudinals and frames, it has been pointed out (reference 13) that the effective width associated with buckling phenomena is not necessarily that based on the load-carrying ability of the sheet, but is proportional to the rate of increase of the apparent stress with the actual stress. If it is assumed that for the present purpose the effective width as given by K and Marguerre's equation is sufficiently accurate, then the apparent stress σ_a is

$$\sigma_a = \frac{2 w_e \sigma_{st}}{b} = \sigma_{st} \sqrt[3]{\frac{\sigma_{cr}}{\sigma_{st}}}$$

The effective width w_e^* for stability is then,

$$\frac{2 w_e^*}{b} = \frac{d\sigma_a}{d\sigma_{st}} = \frac{2}{3} \sqrt[3]{\frac{\sigma_{cr}}{\sigma_{st}}} \quad (2)$$

This equation gives an effective width which is two-thirds of that based on the load-carrying ability of the sheet. However, the influence on the numerical value of ρ_x is quite small. For the specimens tested it was found that the difference was of the order of 3 percent. Although an effective width as given by equation (2) was used in the experimental work, it is felt that either value is sufficiently accurate for all practical purposes.

The amount of sheet acting with the frames is difficult to evaluate by analytical methods. Trial calculations indicated that the best results were obtained if the total width of sheet between frames was used. For this reason it is recommended that the entire width of sheet be used in calculating ρ_y .

The results of the experiments are shown in figure 17 in which $\frac{\sigma_{cr}}{E'}$

is plotted as a function of $\frac{1}{R} \sqrt{\rho_x \rho_y} \sqrt[4]{\rho_x \rho_y / bd}$. In the majority of

tests the frames had a solid rectangular cross section (fig. 1) and were therefore not subject to local instability. When frames, such as the channel section, are subject to local instability, the failing load may be as much as 60 percent lower than that given by the curve of figure 17 since the channel does not develop the strength corresponding to the calculated value of ρ_y . This can be illustrated by considering the behavior of an open-section column subjected to an axial load. Since the initial failure of the frame occurs over a relatively short length, the discussion will be confined to short columns. For columns having stable cross sections, that is, columns which are not subject to local instability, the critical buckling stress is given with reasonable accuracy by the Johnson parabola, namely,

$$\sigma_{\beta} = \sigma_y \left[1 - \frac{\sigma_y^2 l^2}{4\pi^2 CE\rho^2} \right] \quad (3)$$

It has been shown that for columns which fail by local instability (reference 14) the buckling stress σ_c can be calculated by the equation

$$\sigma_c = \sigma_{cc} \left[1 - \frac{\sigma_{cc}^2 l^2}{4\pi^2 CE\rho^2} \right] \quad (4)$$

If the crushing stress σ_{cc} is lower than the yield-point stress the column will not develop the stress given by equation (3), but will fail at some lower stress given by equation (4). For columns which fail by local instability a reduced effective radius of gyration ρ_{eff} can be calculated in such a manner that if ρ_{eff} is substituted in equation (4) the resulting stresses will correspond to the values given by equation (3). This requires that for any column length the value of ρ_{eff} be such that

$$\sigma_c = \sigma_\beta$$

from which it follows that

$$\rho_{\text{eff}} = \left[\frac{\frac{\sigma_y^2 l^2}{4\pi^2 CE}}{\sigma_y - \sigma_{cc} + \frac{\sigma_{cc}^2 l^2}{4\pi^2 CE \rho^2}} \right]^{\frac{1}{2}} \quad (5)$$

It is reasonable to assume that the frame behaves in a similar manner and that a reduced effective radius of gyration can be calculated. In applying this method to three specimens, in which general instability failure was precipitated by local instability of the frames, the resulting values of ρ_{eff} were such as to bring the experimental values in good agreement with the curve of figure 17. The length l was taken as the distance between longitudinals.

The experimentally derived parameter $R/\sqrt{\rho_x \rho_y} \sqrt[4]{bd/\rho_x \rho_y}$ is the ratio between the radius and a quantity having the dimensions of a length defined by $\sqrt{\rho_x \rho_y} \sqrt[4]{\rho_x \rho_y/bd}$. By analogy with the buckling of unstiffened cylinders, it appears that this length is proportional to some extent to an equivalent thickness of the reinforced cylindrical structure.

The failing stress of an unstiffened cylindrical shell of radius R is given by

$$\frac{\sigma_{\text{cr}}}{E'} = \frac{kt}{R} \quad (6)$$

Replacing the thickness t by the radius of gyration ρ of a strip of the shell of unit width, equation (6) can be written in the form

$$\frac{\sigma_{\text{cr}}}{E'} = \frac{k \sqrt{12} \rho}{R} \quad (7)$$

For comparison, the failing stress of the stiffened cylinders can be written in the form

$$\frac{\sigma_{\text{cr}}}{E'} = k' \sqrt{12} \frac{\sqrt{\rho_x \rho_y}}{R} \sqrt[4]{\frac{\rho_x \rho_y}{bd}} \quad (8)$$

where k' is a numerical constant.

By introducing the geometrical mean value $\sqrt{\rho_x \rho_y}$ it can be assumed that the influence of the anisotropy of the structure is approximately taken into account. Then by comparison of equations (7) and (8) an effective radius of gyration can be defined as

$$\rho_e = \frac{k'}{k} \sqrt[4]{\frac{\rho_x \rho_y}{bd}} \sqrt{\rho_x \rho_y} = \varphi \sqrt{\rho_x \rho_y} \quad (9)$$

where $\varphi = \frac{k'}{k} \sqrt[4]{\frac{\rho_x \rho_y}{bd}}$ can be considered as a correction factor to the ratio $\sqrt{\frac{\rho_x \rho_y}{R}}$. Now b/ρ_x is the slenderness ratio of the longitudinal considered as a column between two frames, and similarly d/ρ_x is the slenderness ratio of the frame considered as a column between two longitudinals. If the geometrical mean value of these two slenderness ratios is defined by λ , that is,

$$\lambda = \sqrt{\frac{bd}{\rho_x \rho_y}} \quad (10)$$

then the correction factor can be expressed as

$$\varphi = \frac{k'}{k} \frac{1}{\sqrt{\lambda}}$$

It is evident that if the stiffened shell were to be considered as an equivalent shell, in which all the materials are uniformly distributed, then the appropriate parameter to be used is $\sqrt{\frac{\rho_x \rho_y}{R}}$. The appropriate parameters which enter into the problem of buckling of a truss are the slenderness ratios which appear in the quantity $\lambda = \sqrt{\frac{bd}{\rho_x \rho_y}}$. The fact that the experimentally derived relation involves both parameters, $\sqrt{\frac{\rho_x \rho_y}{R}}$ and λ , indicates that a stiffened cylinder cannot be treated either as an equivalent cylinder of uniform thickness or as a cylindrical truss.

If it is assumed that $k = 0.3$, which is a reasonable average value for unstiffened cylinders in the range of $\frac{\sigma_{cr}}{E}$ involved, and if the values obtained from the experiments are used for k' ; then the numerical

values of ϕ can be calculated. The average slenderness ratio λ varies from 280 to 26 and the values of ϕ corresponding to these limiting cases are $\phi = 0.259$ and $\phi = 0.865$. The lower limit is for a specimen with 10.12-inch longitudinal and 16-inch frame spacing, whereas the upper limit corresponds to a specimen with 2.53-inch longitudinal and 2.0-inch frame spacing. These results indicate that for structures in which the stiffening elements are widely spaced it is necessary that a multiplying factor much smaller than unity be applied to the quantity $\sqrt{\rho_x \rho_y}$, whereas in close spacings the factor is of the order of 1.

If a reinforced cylinder fails by panel instability, the buckling stress should always be lower than the stress necessary to cause a general instability failure. This is obvious because, in order for panel instability to occur, it is necessary that the frame be sufficiently rigid to maintain closely the shape of the structure at the frame. If the frame is not sufficiently rigid, the frame will fail before the panel instability stress is reached, resulting in a general-instability type of failure. The test results shown in figure 18 confirm this statement.

Length Effect

Inasmuch as all the pure-bending specimens had a length to diameter ratio of 2.0, it was necessary to determine whether the failing loads of these specimens were influenced by length. The main purpose of this investigation, therefore was to determine the length to diameter ratio L/D at which the failing load becomes independent of length.

Eight specimens having L/D ratios of 1.2, 1.6, 2.0, and 2.6 were tested, four in which the frame spacing was 2.0 inches and four in which the spacing was 4.0 inches. The spacing of the longitudinals and the diameter were the same for all specimens, 2.56 inches and 20 inches, respectively.

The failing strain as a function of the L/D ratio is shown in figure 19. It is seen that the specimens having L/D ratios of 2 and 2.5 failed at approximately the same strain. As the L/D ratio decreases the failing strain increases somewhat and at an L/D ratio of 1.2 the increase is 12 and 23 percent for the 4- and 2-inch frame spacings, respectively. From these test results it can be concluded that the failing loads of the pure-bending specimens used in the previous experiments were not influenced by length.

Combined Bending and Transverse Shear

In the pure-bending tests, the problem of determining the maximum strain associated with the failing load was relatively simple because of the uniform loading over the length of the specimen. However, when the test specimen is subjected to combined bending and transverse shear, the bending moment and the corresponding strains vary over the length of the specimen. Hence, the method of measuring, over the specimen length, a maximum mean strain at failure and assigning this measured strain to the failing load can no longer be applied. The variation of strain and the end conditions of the specimen make it particularly difficult to associate a particular strain with the failing load. The maximum moment occurs at the fixed end; however, this maximum moment and the corresponding strain cannot be considered as being a measure of the ultimate strength of the cylinder because of the fixed-end conditions.

There are two possible methods of presenting the test data. One method would be to measure the strain at a number of points along the length of the specimen, and then present these measurements as the existing strain condition along the length of the specimen when failure occurred. Another method would be to measure the failing strain at the point at which the first buckle appears during the loading process and to consider this to be indicative of the maximum strain to which the specimen can be subjected before failure occurs.

Both methods have certain disadvantages. The first does not lend itself readily to application in practical design. It is customary, for maximum structural efficiency, to design a reinforced cylindrical structure in such a manner as to keep the stress nearly constant even though the bending moment is variable. This is usually accomplished by taper of the section and also of the effective bending material. From this point of view the second method is preferable. However, the main objection to the second is that the validity of associating the strain condition at a point with the failure of the cylinder may be questionable.

The second method has also one other advantage, namely, for the pure bending failure a parameter has been derived which appears to be satisfactory. In determining the influence of the transverse shear on the maximum strain at failure, it is convenient to have a single value of the strain for combined bending and shear to compare with the strain value for pure bending.

In view of these considerations, the following method of presentation was adopted. It was found that the initial buckle or buckles appeared over a relatively short range, being on the average about 14 inches from the fixed end for the 32-inch-diameter cylinders and 10 inches for the 20-inch-diameter cylinders. For this reason the strain at failure was considered to be the average of the strain measurements over a distance extending from about 4 to 24 inches from the fixed end.

The type of failure in combined bending and shear differs particularly in one respect from that of the pure bending failure. For the combined loading the failure is, in many cases, gradual; that is, the buckles, although extending over several frames and longitudinals, slowly increase in depth and size with increasing load until a sudden collapse occurs with a marked increase in depth and size of the buckle or buckles. In the case of the pure-bending specimens, the original cross-section shape is closely maintained until failure occurs. The failure is particularly violent and accompanied by large and deep buckles with as much as a two-thirds drop in the applied load.

During the early part of the investigation, it appeared from a visual observation that failure of a specimen was either of the bending or the shear type, that is, the beginning of a failure was confined to either a region of maximum compression or a region of maximum shear. The rather definite separation of the regions of failure indicated that when a failure occurred in the compression region the failure was nearly independent of the applied shear and depended primarily on the state of compression strain; whereas, when failure occurred in the region of maximum shear the failure was independent of the state of compression strain and depended only on the applied shear.

These observations were borne out by the experimental results. In figure 20 are plotted the ratios of the compressive strain ϵ/ϵ_0 as a function of VR/M for a number of specimens of both 16-inch and 10-inch radius, where ϵ is the maximum compressive strain value (at the position previously described) for the combined-loading condition, ϵ_0 is the same strain value for pure bending, V is the applied shear, R is the radius of the specimen, and M the bending moment. Since $M = VL$, where L is the distance from the applied shear load to the point where the strain is measured, it is seen that the ratio VR/M is equivalent to R/L . This presentation is merely to indicate that when the failure occurs in the compression region the maximum compressive strain is independent of the applied shear. For these specimens the applied shear load varied from 503 to 1450 pounds for the 16-inch-radius specimens, and for the 10-inch specimens from 710 to 2310 pounds. The minimum moment arm L was limited by the length of the specimen.

In figure 21 are plotted ratios of ϵ/ϵ_0 as a function of V/V_0 for one series of tests, where V_0 is the shear load which causes a pure shear failure and V is the shear load corresponding to ϵ . It is seen from this figure that specimens 116 and 117 failed at the same shear load but widely different values of ϵ (i.e., bending moment). The photographs (figs. 14 and 15) indicate that specimen 116 failed simultaneously by combined bending and shear, whereas specimen 117 failed in shear. It appears from these results that the interaction curve for this type of loading consists essentially of two perpendicular straight lines.

The strains at failure, for the specimens which failed by bending, have been compared with the parameter obtained for the pure-bending failures and are shown in figure 22. The test values follow the same trend as the curve for the pure-bending failures; however, the experimental scatter is somewhat greater than for the pure-bending specimens. It is felt that this scatter is primarily due to the following: (a) the accuracy of the strain measurements depends on the reliability of the electric strain gages and an accuracy greater than 5.0 percent is not to be expected, and (b) adopting a strain value at a constant distance from the fixed end as being indicative of the strain at failure also leads to some inaccuracies.

Pure Torsion

In determining a parameter for predicting the general instability failure in torsion, the same general procedure was followed as was used in reference 5. The variables to be considered are the same as those of the pure-bending problem and can again be divided into two groups, namely, those dealing with the geometry of the structure and those involving the sectional properties of the stiffening elements as well as the sheet covering. The geometrical variables are the longitudinal spacing b , the frame spacing d , the diameter, and the length of the cylinder. The second group of variables includes the section properties of the longitudinals and frames and the thickness of the sheet covering.

A number of specimens were tested in which the geometrical variables b and d were systematically varied while R was kept constant and equal to 16 inches. The results of these tests indicated that τ_{\max} varied as \sqrt{bd} . For the buckling of unstiffened cylinders subjected to pure torsion, the experimental results of reference 15 indicate that, for values of L/R equal to and greater than 3.2, τ_{cr}/E varies approximately as $\left(\frac{t}{R}\right)^{3/4} \sqrt{t/L}$. It was therefore assumed that, for identical values of b , d , ρ_x , and ρ_y , the critical shearing stress for the general instability of a stiffened cylinder would vary as the reciprocal of $\sqrt{bd} R^{3/4}$. In order to verify this assumption, a number of tests were conducted on 10-inch-radius specimens and various values of b and d . A plot of τ_{\max} as a function of $\sqrt{bd} R^{3/4}$ for the 10- and 16-inch specimens is shown in figure 23. These results indicated that the assumption was justified and it was therefore concluded that the parameter for predicting general instability in torsion is of the form

$$\frac{\sqrt{bd} R^{3/4}}{f(\rho_x, \rho_y)}$$

From dimensional reasoning, it follows that the function $f(\rho_x, \rho_y)$ must have the dimensions of the $7/4$ power of a length. The simplest assumption for the function which determines the influence of the section-parameters, ρ_x and ρ_y , is that it depends on only the geometrical mean value $\sqrt{\rho_x \rho_y}$. The parameter therefore appears in the form

$$\sqrt{\frac{bd}{\rho_x \rho_y}} \left(\frac{R}{\sqrt{\rho_x \rho_y}} \right)^{3/4}$$

In checking the validity of this parameter, it is necessary to evaluate the amount of sheet acting with the frames and longitudinals in order to calculate ρ_x and ρ_y . It is quite difficult to evaluate by analytic means the amount of sheet acting with the reinforcing members; trial calculations indicated that the best results were obtained if the total width of sheet was used. For this reason ρ_x and ρ_y were calculated with the entire width of sheet assumed to be effective.

Specimens were also tested in which both the sheet thickness and sectional properties of the longitudinals were varied. The results of all tests are shown plotted in figure 24. It is seen that up to values of 10,000 pounds per square inch all test values scatter closely about a straight line. For higher values of τ_{max} there is a sudden shift in the experimental values. However, the majority of tests again follow a straight line having the same slope as the line corresponding to the lower values of τ_{max} . Since the observed diagonal-tension field varied between about 30° to 50° , it can be shown that for a shear stress of 10,000 pounds per square inch the corresponding tensile stress would be between 20,000 and 23,000 pounds per square inch. It was thought that this tensile stress might be sufficiently close to the proportional limit of the sheet covering to explain the sudden shift in the experimental values. However, an examination of the stress-strain curves indicated that the tensile stress at a shear stress of 10,000 pounds per square inch is well below the proportional limit.

A more desirable presentation of the test data would be to plot

τ_{max}/G_E against $\sqrt{\frac{\rho_x \rho_y}{bd}} \left(\frac{\sqrt{\rho_x \rho_y}}{R} \right)^{3/4}$ since τ_{max}/G_E corresponds

to the shearing strain r . Such a presentation would be more general and would allow for materials of different physical properties or for changes in the physical properties above the proportional limit. It had not been realized at the beginning of the test program that it would be desirable to obtain a measure of τ/G_E at failure. For this reason angular deformations were measured on only a number of specimens. Not enough measurements are available to make such a plot. A plot of τ_{\max}/E as a

function of $\sqrt{\frac{\rho_x \rho_y}{bd}} \left(\sqrt{\frac{\rho_x \rho_y}{R}} \right)^{3/4}$ is given in figure 25. The value of E in this figure corresponds to that of the sheet covering and was taken as 10^7 pounds per square inch, since this corresponded closely to the actual test values obtained for the sheet.

Combined Bending and Torsion

For a combined-loading condition it would be a difficult and lengthy task to obtain experimentally a parameter describing the failure of a stiffened cylinder. For this reason the ultimate stresses at failure were presented in the form of interaction curves; that is, σ/σ_0 was plotted as a function of τ/τ_0 , where σ is the normal compression stress at failure for combined loading and σ_0 is the same stress at failure for pure bending, and similarly, τ and τ_0 are the shearing stresses at failure for combined loading and pure torsion, respectively. The shearing stresses were computed by the equation

$$\tau = \frac{M}{2 AT} \quad (11)$$

Two sets of data are shown. The first set (fig. 26) corresponds to stresses as measured by the resistance strain gages and the second set (fig. 27), to the stresses as obtained from the dial-gage measurements. In either case a considerable amount of scatter is evident. The interaction equations of the form

$$\left(\frac{\sigma}{\sigma_0} \right)^2 + \left(\frac{\tau}{\tau_0} \right)^2 = 1 \quad (12)$$

and

$$\frac{\sigma}{\sigma_0} + \left(\frac{\tau}{\tau_0} \right)^2 = 1 \quad (13)$$

are compared with the experimental results. Figure 26 indicates that for the resistance-strain-gage measurements about two-thirds of the test values lie fairly close to the curve of equation (13); whereas the majority of the dial-gage measurements scatter about the curve of equation (12).

SUMMARY OF DESIGN CURVES AND EQUATIONS

A summary of the design curves and equations for the conditions studied is as follows:

(1) Pure bending

For the ultimate longitudinal strain at failure it is recommended that the lower curve of figure 18 be used, or be calculated from the equation of this curve, which is

$$\frac{\sigma_{cr}}{E'} = \frac{k_1 \sqrt{\rho_x \rho_y}}{R} + \sqrt{\frac{\rho_x \rho_y}{bd}}$$

where $k_1 = 4.13$. The strain values thus obtained correspond to the lower limit of the experimental strain values at failure.

(2) Combined bending and transverse shear

For this loading two types of failure are possible - a bending failure in the zone of maximum compression or a shear failure in the zone of maximum shear. It is recommended that these failures be checked in the following manner:

(a) Bending failure. - The lower curve of figure 18 or the equation of this curve as given above.

(b) Shear failure. - The possibility of a shear failure can be checked by calculating the maximum shear stress and comparing this shear stress with the ultimate shear stress of figure 24. The four shear failures listed in table II have been compared with the curve of figure 24; three are in fair agreement and one (specimen 117) failed at a shear stress of approximately 25 percent less than that given by the curve of figure 24.

(3) Combined bending and torsion

For this loading the equation

$$\frac{\sigma}{\sigma_o} + \left(\frac{\tau}{\tau_o} \right)^2 = 1$$

is recommended.

CONCLUSIONS

As the result of an investigation of the general instability of stiffened metal cylinders, parameters were evolved which make it possible to obtain an estimate of the stress at which general instability will occur for any given stiffened metal structure of circular cross section. It is felt that both the geometrical quantities and sectional properties of the structural members were varied over a sufficient range to establish, in general, the validity of the parameters. Because of the catastrophic nature of a general instability failure it is recommended that ample margins of safety be allowed in an airplane structure in which this type of failure might occur.

No attempt was made to give a theoretical treatment of the general instability problem because of the nonlinearity of the buckling problem of stiffened cylinders. The parameters presented for predicting the ultimate strength of stiffened metal cylinders subjected to pure bending and pure torsion were based on an analysis of the experimental results and on the existing theory of unstiffened metal cylinders. This method was preferred over that of a linearized theory which cannot correctly describe the behavior of the structure. The results of a linear theory would have to be modified and corrected to bring it into agreement with the experimental observations, and thus the theory would immediately be rendered an empirical method.

Guggenheim Aeronautics Laboratory,
California Institute of Technology,
Pasadena, Calif., August 1, 1944.

REFERENCES

1. Guggenheim Aeronautical Laboratory, California Institute of Technology: Some Investigations of the General Instability of Stiffened Metal Cylinders. I - Review of Theory and Bibliography. NACA TN No. 905, 1943.
2. Guggenheim Aeronautical Laboratory, California Institute of Technology: Some Investigations of the General Instability of Stiffened Metal Cylinders. II - Preliminary Tests of Wire-Braced Specimens and Theoretical Studies. NACA TN No. 906, 1943.
3. Guggenheim Aeronautical Laboratory, California Institute of Technology: Some Investigations of the General Instability of Stiffened Metal Cylinders. III - Continuation of Tests of Wire-Braced Specimens and Preliminary Tests of Sheet-Covered Specimens. NACA TN No. 907, 1943.

4. Guggenheim Aeronautical Laboratory, California Institute of Technology: Some Investigations of the General Instability of Stiffened Metal Cylinders. IV - Continuation of Tests of Sheet-Covered Specimens and Studies of the Buckling Phenomena of Unstiffened Circular Cylinders. NACA TN No. 908, 1943.
5. Guggenheim Aeronautical Laboratory, California Institute of Technology: Some Investigations of the General Instability of Stiffened Metal Cylinders. V - Stiffened Metal Cylinders Subjected to Pure Bending. NACA TN No. 909, 1943.
6. Guggenheim Aeronautical Laboratory, California Institute of Technology: Some Investigations of the General Instability of Stiffened Metal Cylinders. VI - Stiffened Metal Cylinders Subjected to Combined Bending and Transverse Shear. NACA TN No. 910, 1943.
7. Guggenheim Aeronautical Laboratory, California Institute of Technology: Some Investigations of the General Instability of Stiffened Metal Cylinders. VII - Stiffened Metal Cylinders Subjected to Combined Bending and Torsion. NACA TN No. 911, 1943.
8. Dunn, Louis G.: Some Investigations of the General Instability of Stiffened Metal Cylinders. VIII - Stiffened Metal Cylinders Subjected to Pure Torsion. NACA TN No. 1197, 1947.
9. Hoff, N. J.: Instability of Monocoque Structures in Pure Bending. Jour. Roy. Aero. Soc., vol. 42, April 1938, pp. 291-346.
10. Taylor, J. L.: Stability of a Monocoque in Compression. R. & M. No. 1679, British A.R.C., 1935.
11. Dschou, Dji, Djuän.: Die Druckfestigkeit versteifer zylindrischer Schalen. Luftfahrtforschung, vol. 11, no. 8, Feb. 1935, pp. 223-234.
12. Hoff, N. J.: General Instability of Monocoque Cylinders. Jour. Aero. Sci., vol. 10, April 1943, pp. 105-114; 130.
13. Cox, H. L.: Stress Analysis of Thin Metal Construction. Jour. Roy. Aero. Soc., vol. 7, March 1940, pp. 231-282.
14. Lundquist, Eugene, E.: Local Instability of Centrally Loaded Columns of Channel Section and Z-Section. NACA TN No. 722, 1939.
15. Donnel, L. H.: Stability of Thin-Walled Tubes under Torsion. NACA Rep. No. 479, 1933.

TABLE I

Pure-Bending Tests of Longitudinal - Frame Combinations

[All Longitudinals S_1]

Test	Frame No.	Sheet Thick. (in.)	Long. Spacing. b (in.)	Frame Spacing. d (in.)	Radius (in.)	Max. Unit Strain	$\sqrt[4]{bd}$	P_x	P_y	$\frac{4}{\sqrt{(P_x P_y)^3}}$	$\frac{\sqrt[4]{bd}}{\sqrt{(P_x P_y)^3}} R$	Type of Failure
25	F ₅	.010	2.53	8	15.92	.00170	2.120	.1168	.02335	.01145	2822	General Instability
26			2.53	4		.00208	1.783	.1165	.02677	.01320	2150	" "
27			2.53	2		.00288	1.500	.1165	.02836	.01380	1730	" "
28			2.53	16		.00130	2.520	.1169	.01875	.01010	3970	Started by Panel Instability Final Failure General Instability
29			5.06	16		.00092	2.998	.1160	.01875	.01023	4660	Panel Instability
30			5.06	8		.00140	2.520	.1166	.02335	.01190	3370	General Instability
31			5.06	4		.00190	2.120	.1169	.02677	.01325	2550	" "
32			5.06	2		.00256	1.783	.1167	.02836	.01380	2060	" "
34			10.12	16		.00088	3.560	.1110	.01875	.00975	5820	Started by Panel Instability Final Failure General Instability
35			10.12	8		.00120	2.998	.1120	.02335	.01160	4120	General Instability
36			10.12	4		.00164	2.520	.1122	.02677	.01280	3135	" "
37			10.12	2		.00200	2.120	.1117	.02836	.01330	2540	" "
38			5.06	1		.00283	1.500	.1164	.02801	.01360	1755	" "
39		.010	2.53	1		.00326	1.261	.1170	.02801	.01360	1478	" "



TABLE I (CONTD)

Test	Frame No.	Sheet Thick. (in.)	Long. Spacing, b (in.)	Frame Spacing, d (in.)	Radius (in.)	Max. Unit Strain	$\sqrt[4]{bd}$	ρ_x	ρ_y	$\sqrt[4]{\frac{\rho_x \rho_y}{xy}}$	$\sqrt[4]{\frac{bd}{\rho_x \rho_y}}$	Type of Failure
40	F ₅	.015	2.53	16	15.92	.00104	2.520	.1175	.01723	.00955	4210	Panel Instability
41			2.53	8		.00182	2.120	.1180	.02176	.01140	2960	General Instability
42			2.53	4		.00215	1.783	.1184	.02608	.01310	2168	" "
43			2.53	2		.00280	1.500	.1184	.02879	.01410	1696	" "
44			5.06	16		.00066	2.998	.1140	.01723	.00935	5110	Panel Instability
45			5.06	8		.00146	2.520	.1150	.02176	.01120	3580	General Instability
46			5.06	4		.00167	2.120	.1151	.02608	.01285	2630	" "
47			5.06	2		.00249	1.783	.1151	.02879	.01380	2060	" "
48			10.12	16		.00048	3.560	.104	.01723	.00870	6520	Panel Instability
49			10.12	8		.00128	2.998	.1049	.02176	.01050	4540	General Instability
50			10.12	4		.00150	2.520	.1060	.02608	.01195	3360	" "
51	F ₅	.015	10.12	2	15.92	.00250	2.120	.1061	.02879	.01300	2600	" "
52	F ₁	.010	2.53	16	16.00	.00180	2.520	.1168	0.1288	.0430	938	Panel Instability
53			2.53	8		.00216	2.120	.1165	0.0811	.0303	1120	" "
54			2.53	4		.003732	1.783	.1168	0.0982	.03500	812	General Instability

TABLE I (CONCLUDED)

Test	Frame No.	Sheet Thick. (in.)	Long. Spacing, b (in.)	Frame Spacing, d (in.)	Radius (in.)	Max. Unit Strain	$\sqrt[4]{bd}$	ρ_x	ρ_y	$\sqrt[4]{\frac{\rho_x \rho_y}{R}}$	$\frac{bd}{R^2}$	Type of Failure
55	F ₁	.010	2.53	2	16	.004775	1.500	.1168	.11000	.0378	636	General Instability
56			5.06	16		.00090	2.998	.1150	.06330	.0250	1920	Panel Instability
57				8		.00228	2.520	.1150	.08110	.0300	1345	Panel Instability
58				4		.004350	2.120	.1160	.09820	.0350	965	General Instability
59	F ₁			2		.006154	1.783	.1165	.11000	.0378	742	" "
60	F ₆			8		.00243	2.520	.1270	.06340	.0251	1715	Panel Instability
61				4		.004927	2.120	.1270	.06400	.0254	1245	General Instability
62			5.06	2			1.783		.06180			Tension Failure
63			2.53	4		.004045	1.783	.1278	.06400	.0255	1045	General Instability
64	F ₆		2.53	2	16	.005100	1.500	.1278	.06180	.0247	905	" "
65	F ₅		2.61	4	10	.003150	1.798	.1163	.02677	.0132	1362	" "
66			2.61	2		.004200	1.510	.1168	.02836	.0138	1095	" "
67			5.22	4		.002950	2.175	.1165	.02677	.0132	1650	" "
68			5.22	2		.003750	1.798	.1166	.02836	.0138	1300	" "
73			2.61	4		.003200	1.798	.1162	.02677	.0132	1365	" "
74	F ₅	.010	2.61	2	10	.004400	1.510	.1164	.02836	.0138	1095	" "

all sheet = .010 in.

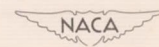
all longitudinals S_1

TABLE II

Test	Long Spacing, b (in.)	Frame Spacing, d (in.)	Radius (in.)	Ultimate Applied Shear (lb)	Moment arm - to fixed end (in.)	Strain at Failure	\sqrt{bd}	P_x	P_y	$\sqrt{(P_x P_y)^2}$	$\sqrt{\frac{bd}{(P_x P_y)^2}}$	$\sqrt{\frac{P_x P_y}{bd}}$	Type of Failure
75	5.06	8	16	1057	128	.00161	2.52	.1167	.02335	.0119	3390	2.95×10^{-4}	Gen. Instability
76	"	"	"	1050	116	.00153	"	.1167	.02335	.0119	3390	2.95 "	"
77	"	"	"	1450	92	.001516	"	.1167	.02335	.0119	3390	2.95 "	"
78	"	"	"	995	116	.00151	"	.1167	.02335	.0119	3390	2.95 "	"
79	"	2"	"	2000	128	.00270	1.785	.1172	.02836	.0138	2070	4.83 "	"
80	"	"	"	1850	107	.00211	"	.1170	.02836	.0138	2070	4.83 "	"
81	"	"	"	2175	86	.00242	"	.1170	.02836	.0138	2070	4.83 "	"
82	"	"	"	2070	64	.00189	"	.1170	.02836	.0138	2070	4.83 "	"
83	10.12	4	"	563	128	.00154	2.52	.1117	.02677	.0128	3150	3.18 "	"
84	"	2	"	825	128	.00212	2.12	.1129	.02836	.0135	2510	3.98 "	"
85	"	"	"	915	104	.00195	"	.1127	.02836	.0134	2530	3.95 "	"
86	"	"	"	915	80	.00218	"	.1130	.02836	.0135	2510	3.98 "	"
87	"	"	"	929	66.5	.00213	"	.1130	.02836	.0135	2510	3.98 "	"
88	5.06	4	"	2115	80	.00216	"	.1170	.02677	.0132	2570	3.89 "	"
89	"	"	"	1910	66.5	.00187	"	.1169	.02677	.0132	2570	3.89 "	"
90	"	"	"	1212	128	.00209	"	.1170	.02677	.0132	2570	3.89 "	"

NACA TN No. 1198

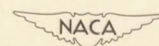
25



all sheet = .010 in.
all longitudinals S_1

TABLE II (CONT'D)

Test	Long Spacing, b (in.)	Frame Spacing, d (in.)	Radius (in.)	Ultimate Applied Shear (lb)	Moment arm - to fixed end (in.)	Strain at Failure	$\sqrt[4]{bd}$	P_x	P_y	$\sqrt[4]{(P_x P_y)^3}$	$\sqrt[4]{bd} R / \sqrt[4]{(P_x P_y)^3}$	$\sqrt[4]{(P_x P_y)^3} / bd$	Type of Failure
91	5.06	4	16	1331	116	.00194	2.12	.1169	.02677	.0132	2570	3.89×10^{-4}	Gen. In-stability
92	"	8	"	503	194	.00152	2.52	.1167	.02335	.0119	3390	2.95 "	"
93	"	"	"	1353	74	.00135	"	.1166	"	.0119	3390	2.95 "	"
94	2.62	"	10"	960	114	.00174	-	-	-	-	-	-	Panel in-stability
95	"	"	"	1283	88.4	.00290	2.14	.1165	.02335	.0119	1800	5.55 "	Gen. In-stability
96	"	"	"	1711	65	.00265	"	.1166	"	.0119	1800	5.55 "	"
97	"	"	"	2900	40.5	.00207	-	-	-	-	-	-	Shear
98	"	4	"	1310	113	.00340	1.80	.1163	.02677	.0132	1360	7.35 "	Gen. In-stability
99	"	"	"	1660	88.4	.00330	"	.1164	"	.0132	1360	7.35 "	"
100	"	"	"	2250	65	.00270	-	-	-	-	-	-	Bending-Shear
101	"	"	"	3300	40.5	.00280	-	-	-	-	-	-	Shear
102	2.53	2	16	2480	137	.00282	1.50	.1160	.02836	.0137	1750	5.71 "	Gen. In-stability
103	"	"	"	2860	112.4	.00277	"	.1160	"	.0137	1750	5.71 "	"
104	"	"	"	4200	89	.00343	"	.1157	"	.0137	1750	5.71 "	"
105	"	"	"	4500	65.1	.00218	-	-	-	-	-	-	Shear
106	2.62	"	10	1490	113	.00396	1.51	.1161	.02836	.0138	1090	9.17 "	Gen. In-stability



all sheet = .010 in.

all longitudinals S₁

TABLE II (CONT'D)

Test	Long Spacing, b (in)	Frame Spacing, d (in)	Radius (in.)	Ultimate Applied Shear (lb)	Moment arm - to fixed end (in)	Strain at Failure	\sqrt{bd}	P _x	P _y	$\sqrt[4]{(P_x P_y)^3}$	$\frac{\sqrt{bd} R}{(P_x P_y)^3}$	$\frac{\sqrt[4]{(P_x P_y)^3}}{bd} R$	Type of Failure
107	2.62	2	10	2760	65	.00450	1.51	.1160	.02836	.0137	1100	9.10x10 ⁻⁴	Gen. In-stability
108	"	"	"	4270	40.5	.00398	"	.1161	"	.0138	1090	9.17 "	"
109	5.24	8	"	450	113	.00186	2.54	.1162	.02335	.0119	2130	4.69 "	"
110	"	"	"	1470	40.5	.00242	2.54	.1166	.02335	.0119	2130	4.69 "	"
111	"	4	"	660	113	.00251	2.14	.1170	.02677	.0132	1620	6.17 "	"
112	"	"	"	1780	40.5	.00290	"	.1169	"	.0132	1620	6.17 "	"
113	"	"	"	930	88.4	.00265	"	.1169	"	.0132	1620	6.17 "	"
114	2.53	"	16"	1900	137	.00216	1.785	.1162	"	.0132	2160	4.63 "	"
115	"	"	"	2010	112.4	.00194	"	.1163	"	.0132	2160	4.63 "	"
116	"	"	"	2400	89	.00217	"	.1162	"	.0132	2160	4.63 "	"
117	"	"	"	2450	65.3	.00136	-	-	-	-	-	-	Shear
118	5.24	2	10	710	113	.00360	1.80	.1170	.02836	.0138	1300	7.69 "	Gen. In-stability
119	"	"	"	990	88.4	.00364	"	.1170	"	.0138	1300	7.69 "	"
120	"	"	"	1460	65	.00353	"	.1169	"	.0138	1300	7.69 "	"
121	"	"	"	2310	40.5	.00374	"	.1170	"	.0138	1300	7.69 "	"
122	2.62	1	"	1665	113	.00525	1.27	.1159	.02801	.0136	930	10.75 "	"
123	"	"	"	2140	88.4	.00492	"	.1160	"	.0136	930	10.75 "	"
124	"	"	"	3220	65	.00481	"	.1160	"	.0136	930	10.75 "	"

NACA TN No. 1198



TABLE III

SPEC. NO.	STIFF. NO.	FRAME NO.	b (in.)	d (in.)	\sqrt{bd}	R (in)	$R^{3/4}$	$\sqrt{bd} R^{3/4}$	p_x	p_y	$(p_x p_y)^{7/8}$	$\sqrt{\frac{p_x p_y}{bd}} \left[\frac{R^{3/4}}{R} \right] \times 10^5$	t (in)	M_{Tmax}	T_{max}
149	S ₂	F ₅	5.12	4	4.52	16	8.0	36.1	.1061	.0269	.00594	16.45	.010	10.70	6600
162	S ₂		2.56	4	3.20	16	8.0	25.6	.1169	.0269	.00648	25.3	.010	13.00	8100
171	S ₁		2.56	4	3.20	16	8.0	25.6	.1145	.0269	.00636	24.82	.010	11.85	7380
175	S ₁		2.56	8	4.52			36.1	.1145	.0234	.00563	15.6	.010	8.00	4970
176	S ₁		2.56	2	2.26			18.075	.1145	.0285	.00670	37.05	.010	15.80	9840
177	S ₁		5.12	16	8.98			71.9	.0967	.01732	.00373	5.19	.015	5.00	2070
178	S ₁		5.12	8	6.36			50.9	.0967	.0218	.00455	8.94	.015	7.50	3110
179	S ₁		5.12	4	4.52			36.1	.0967	.0262	.00536	14.8	.015	10.90	4510
180	S ₁		5.12	2	3.20			25.6	.0967	.0289	.00584	22.8	.015	17.00	7040
181	S ₁		5.12	16	8.98			71.9	.0915	.01525	.00318	4.42	.020	7.30	2270
182	S ₁		5.12	8	6.36			50.9	.0915	.0202	.00406	7.97	.020	9.25	2890
183	S ₁		5.12	4	4.52			36.1	.0915	.0251	.00491	13.6	.020	13.50	4190
184	S ₁		5.12	2	3.20			25.6	.0915	.0289	.00556	21.7	.020	23.35	7010
185	S ₁		5.24	8	6.48	10	5.62	37.4	.0961	.0218	.00453	12.1	.015	3.80	4025
186	S ₁		5.24	4	4.58	10	5.62	25.8	.0961	.0262	.00533	20.6	.015	6.30	6670
187	S ₁		5.24	2	3.24	10	5.62	18.2	.0961	.0289	.00581	31.9	.015	8.90	9500
189	S ₁		10.24	32	18.1	16	8.0	144.9	.0895	.0143	.00296	2.04	.010	1.30	810
190	S ₁		10.24	16	12.8	16	8.0	102.5	.0899	.0188	.00376	3.67	.010	2.50	1560

TABLE III (CONCLUDED)

SPEC. NO.	STIFF. NO.	FRAME NO.	b (in.)	d (in.)	\sqrt{bd}	R (in.)	$R^3/4$	$\sqrt{bd} R^3/4$	ρ_x	ρ_y	$(\rho_x \rho_y)^{1/8}$	$\frac{(\rho_x \rho_y)^{1/8}}{b d} \left[\frac{\rho_x \rho_y}{R} \right]^{3/4} \times 10^5$	t (in.)	M_{Tmax}	I_{max}
191	S ₁	F ₅	10.24	8	8.98	16	8.0	71.9	.0899	.0234	.00455	6.33	.010	4.10	2550
192	S ₁		10.24	4	6.36	16	8.0	50.9	.0899	.0269	.00514	10.1	.010	6.76	4210
193	S ₁		2.56	8	4.52	16	8.0	18.075	.1145	.0285	.0067	37.05	.010	16.00	9940
194	S ₃		5.24	8	6.48	10	5.62	37.4	.0947	.0228	.00466	12.45	.0115	2.90	4010
195	S ₃		5.24	4	4.58			25.8	.0947	.0266	.00533	20.65	.0115	4.95	6780
196	S ₃		5.24	2	3.24			18.2	.0947	.0287	.00571	31.30	.0115	6.70	9270
197	S ₂		2.62	8	4.58			25.8	.1166	.0228	.00558	21.60	.0115	5.10	7050
198	S ₂		2.62	4	3.24			18.2	.1166	.0266	.00641	35.20	.0115	7.40	10250
199	S ₂		2.62	2	2.29			12.85	.1166	.0287	.00683	53.20	.0115	9.00	12450
200	S ₂		2.62	2	2.29			12.85	.1152	.0285	.00673	52.40	.010	7.90	12560
201	S ₂		2.62	1	1.62			9.05	.1152	.0281	.00665	73.50	.010	11.50	18290
202	S ₂	↓	2.62	1	1.62			9.05	.1152	.0281	.006836	75.7	.020	24.00	19100
203	S ₁	F ₇	2.62	8	4.58			25.8	.1136	.0385	.00866	33.6	.0115	7.00	9690
204	S ₁		2.62	4	3.24			18.2	.1136	.0428	.00950	52.2	.0115	10.50	14540
205	S ₁		2.62	2	2.29			12.85	.1136	.0436	.0966	75.2	.0115	13.90	19200
206	S ₁		2.62	8	4.58			25.8	.1110	.0316	.00708	27.5	.0200	10.50	8350
207	S ₁		2.62	4	3.24			18.2	.1110	.0415	.0092	50.5	.020	14.85	11820
208	S ₁	↓	2.62	2	2.29	↓	↓	12.85	.1110	.0453	.0097	75.5	.020	22.0	17500
209	S ₁		2.62	3	2.8			15.72	.1110	.0435	.0965	61.5	.020	18.90	15000

TABLE IV
COMBINED BENDING AND TORSION

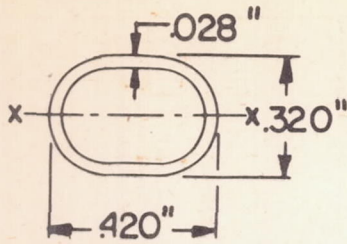
Specimen	Sheet thickness (in.)	Radius (in.)	Frame	Stiffener	Frame spacing (in.)	Longitudinal spacing (in.)	Torsion bending	Ultimate bending moment (in.-lb)	Ultimate torsional moment (in.-lb)	Compressive strain at failure (in./in.)	Shear stress at failure (lb/sq in.)
149	.010	16	F ₅	S ₂	4	5.08	Torsion	0	1070x10 ²	5.60x10 ⁻⁴	6650
150	↓	↓	↓	↓	↓	↓	5/1	216x10 ²	1080	7.64	6710
151	↓	↓	↓	↓	↓	↓	3/1	287	860	7.12	5340
152	↓	↓	↓	↓	↓	↓	2/1	472	945	10.70	5870
153	↓	↓	↓	↓	↓	↓	1/1	770	770	13.5	4780
154	↓	↓	↓	↓	↓	↓	1/1.5	900	600	14.6	3730
155	↓	↓	↓	↓	↓	↓	1/2	1000	500	18.6	3110
156	↓	↓	↓	↓	↓	↓	1/2.5	1175	470	18.05	2920
157	↓	↓	↓	↓	↓	↓	1/3	1150	385	16.2	2390
158	↓	↓	↓	↓	↓	↓	1/3.5	1210	355	16.7	2200
159	↓	↓	↓	↓	↓	↓	Bending	1400	0	16.0	0
160	↓	↓	↓	↓	↓	↓	1/1.5	875	583	14.4	3620
161	↓	↓	↓	↓	↓	5.08	1/5	1200	240	16.2	1490
162	↓	↓	↓	↓	↓	2.53	Torsion	0	1300	2.12	8080
163	↓	↓	↓	↓	↓	↓	1/1	820	820	7.00	5100
164	↓	↓	↓	↓	↓	↓	2/1	575	1150	5.27	7150



TABLE IV (CONCLUDED)

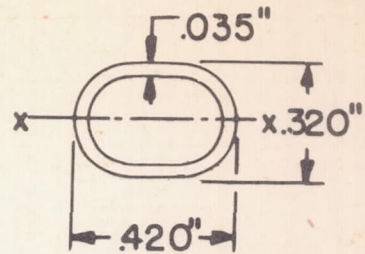
Specimen	Sheet thickness (in.)	Radius (in.)	Frame	Stiffener	Frame spacing (in.)	Longitudinal spacing (in.)	Torsion bending	Ultimate bending moment $\times 10^4$ (in.-lb)	Ultimate torsional moment $\times 10^4$ (in.-lb)	Compressive strain at failure $\times 10^{-4}$ (in./in.)	Shear stress at failure (lb/sq in.)
165	.010	16	F ₅	S ₁	4	2.53	1/2	1390	695	10.95	4320
166	↓	↓	↓	↓	↓	↓	1/3	1900	633	14.00	3930
167	↓	↓	↓	↓	↓	↓	1/5	2540	508	17.6	3160
168	↓	↓	↓	↓	↓	↓	1/2	1600	800	12.5	4970
169	↓	↓	↓	↓	↓	↓	1/1	1050	1050	9.4	6520
170	↓	↓	↓	S ₂	↓	↓	2/1	550	1100	5.25	6840
171	↓	↓	↓	S ₁	↓	↓	Torsion	0	1185	1.85	7360
172	↓	↓	↓	↓	↓	↓	1/1	900	900	9.75	5590
173	↓	↓	↓	↓	↓	↓	1/2	1280	645	14.10	4010
174	.010	16	F ₅	S ₁	4	2.53	1/4	1880	460	21.40	2860





STIFFENER-S₁

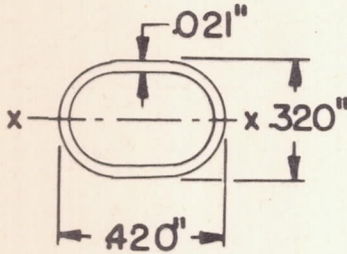
Area=0.0324 $I_{xx}=0.000374$



STIFFENER-S₂

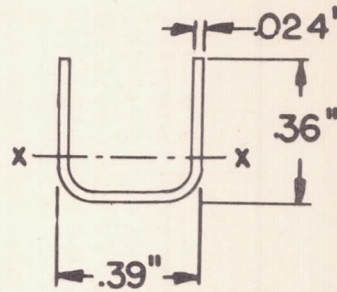
Area=0.0368 $I_{xx}=0.000407$

Note: All drawings are twice actual size



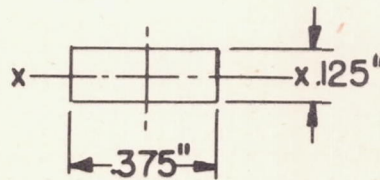
STIFFENER-S₃

Area=0.02295 $I_{xx}=0.000326$



FRAME-F₁

Area=0.02355 $I_{xx}=0.00031194$



FRAME-F₇

Area=0.04688 $I_{xx}=6.108 \times 10^{-5}$

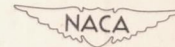
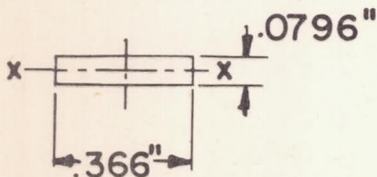
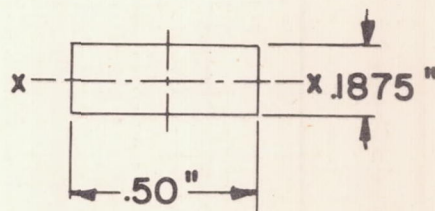


FIGURE 1.



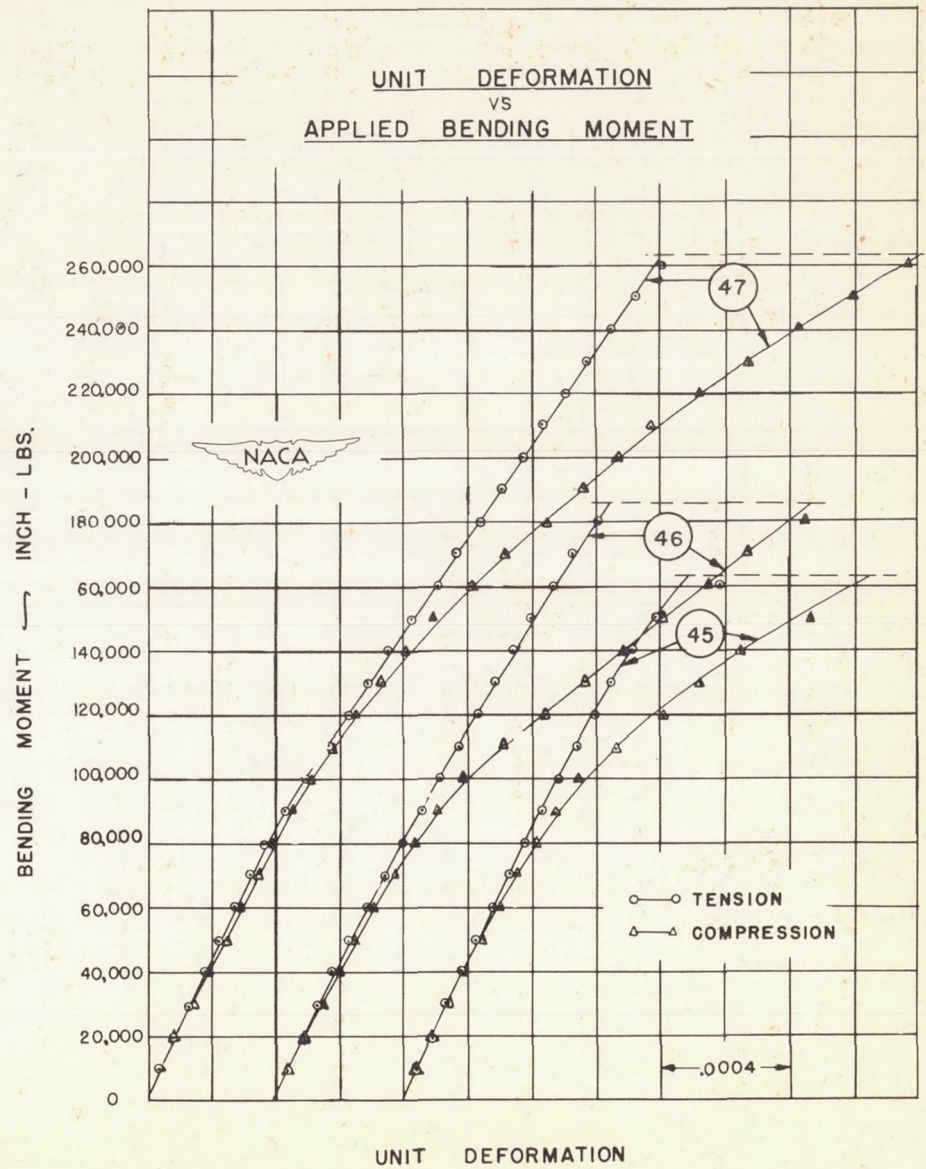
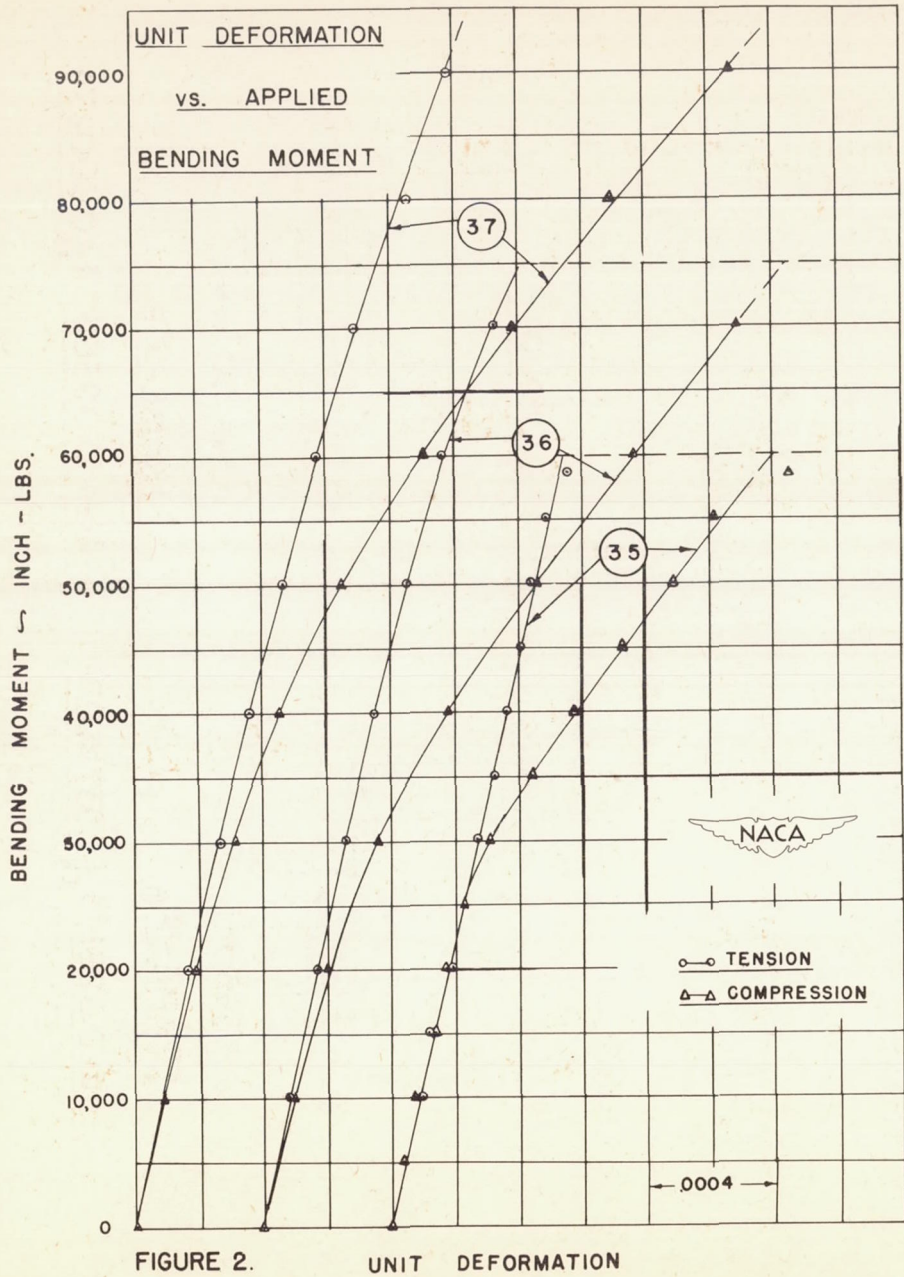
FRAME-F₅

Area=0.0291 $I_{xx}=1.537 \times 10^{-5}$



FRAME-F₆

Area=0.09365 $I_{xx}=0.000274$



SPECIMEN NO. 159
BENDING

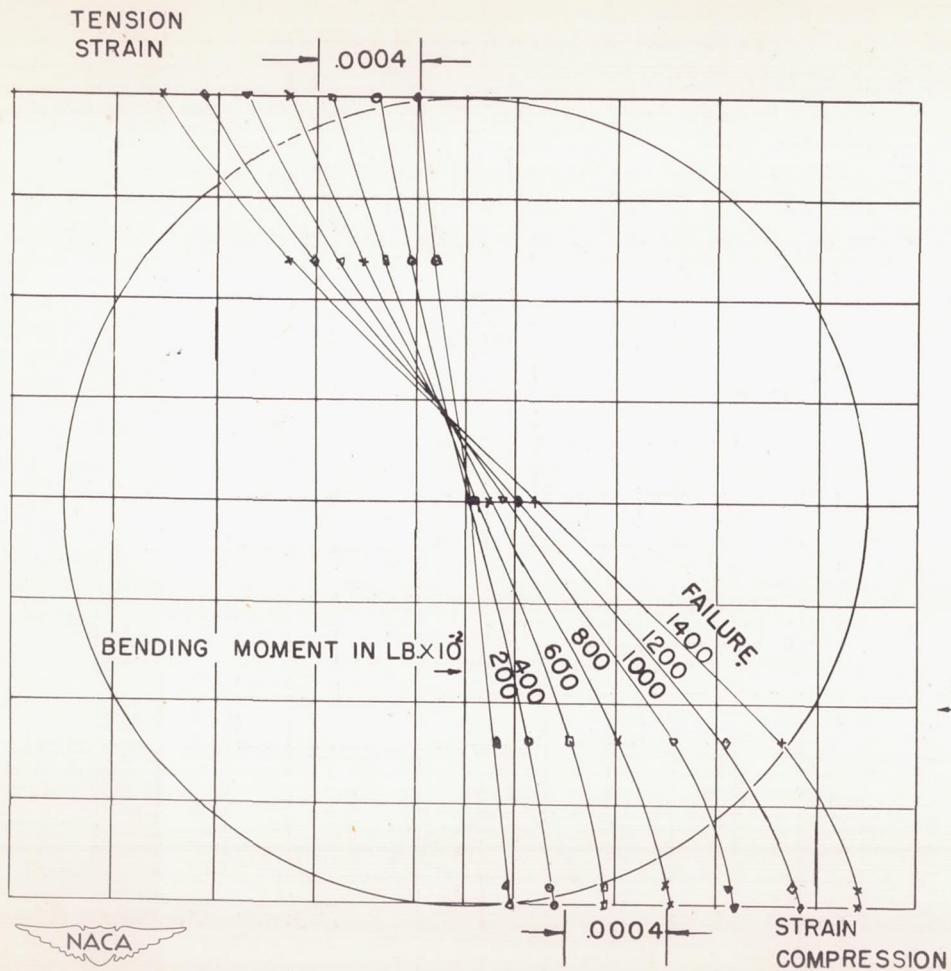


FIGURE 4.

- 800 lbs shear
- ▼ 1200 " "
- 1900 " " (failure)

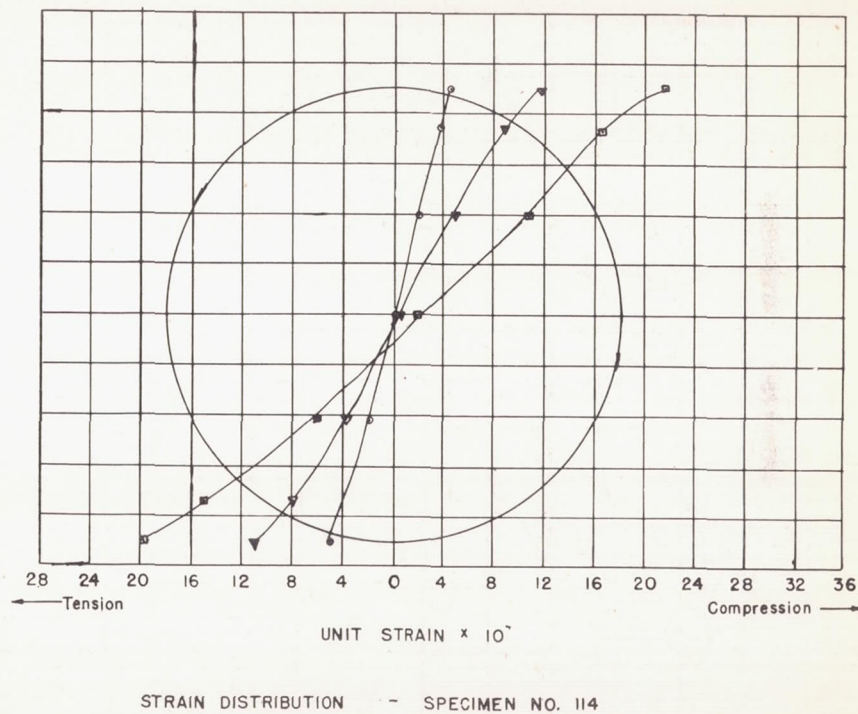
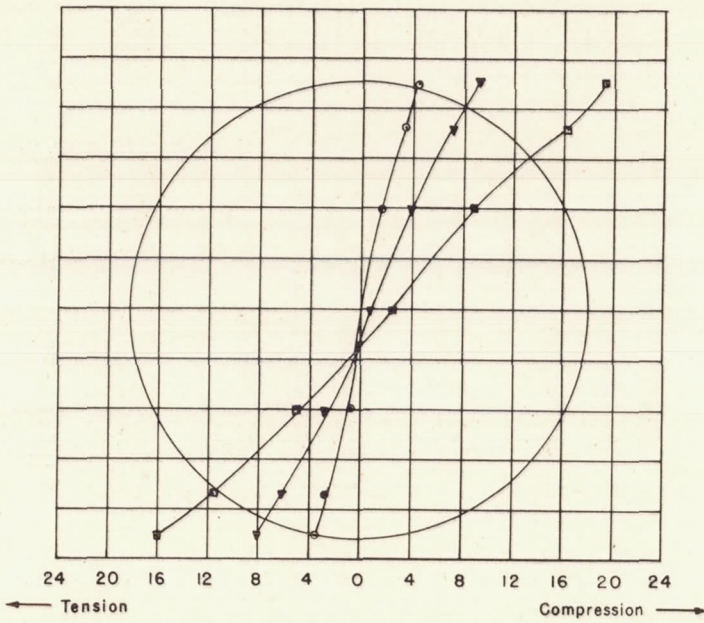


FIGURE 5.

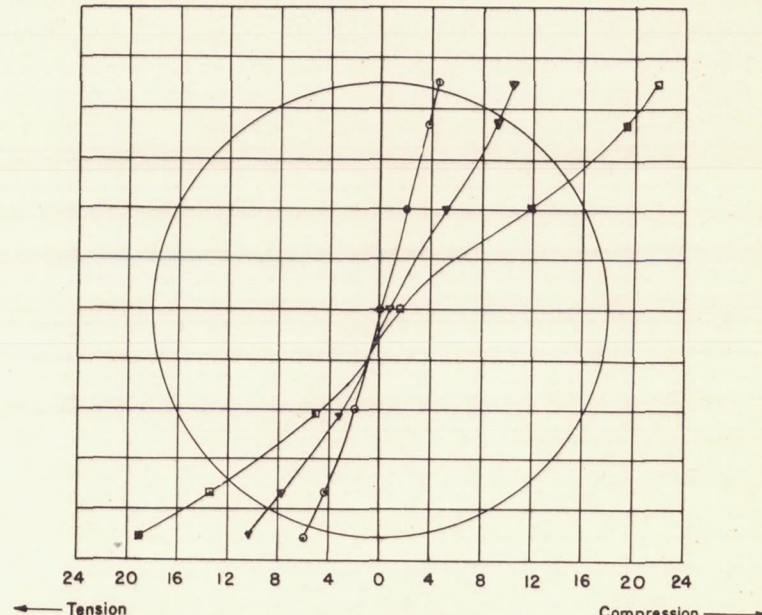
○ 600 lbs shear
 ▼ 1200 " "
 □ 2010 " " (failure)

○ 900 lbs shear
 ▼ 1600 " "
 □ 2400 " " (failure)



NACA
 UNIT STRAIN $\times 10^4$
 STRAIN DISTRIBUTION — SPECIMEN NO. 115

FIGURE 6.



NACA
 UNIT STRAIN $\times 10^4$
 STRAIN DISTRIBUTION — SPECIMEN NO. 116

FIGURE 7.

SPECIMEN NO. 161
 TORSION $\frac{1}{5}$
 BENDING $\frac{1}{5}$

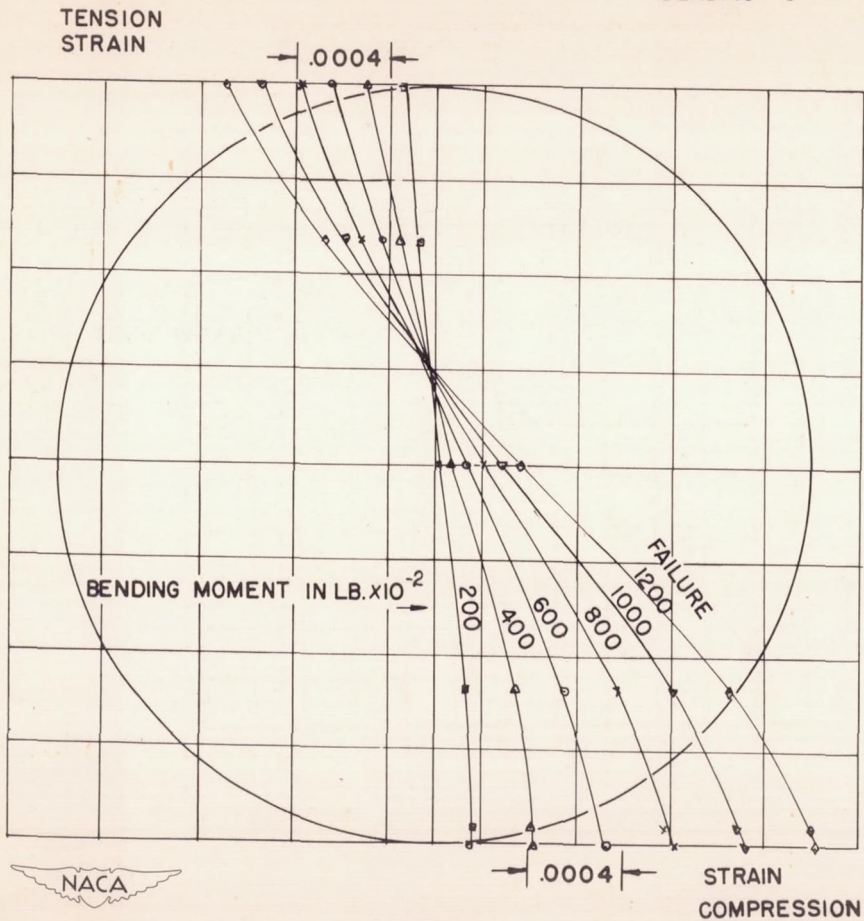


FIGURE 8.

SPECIMEN NO. 153
 TORSION $\frac{1}{1}$
 BENDING $\frac{1}{1}$

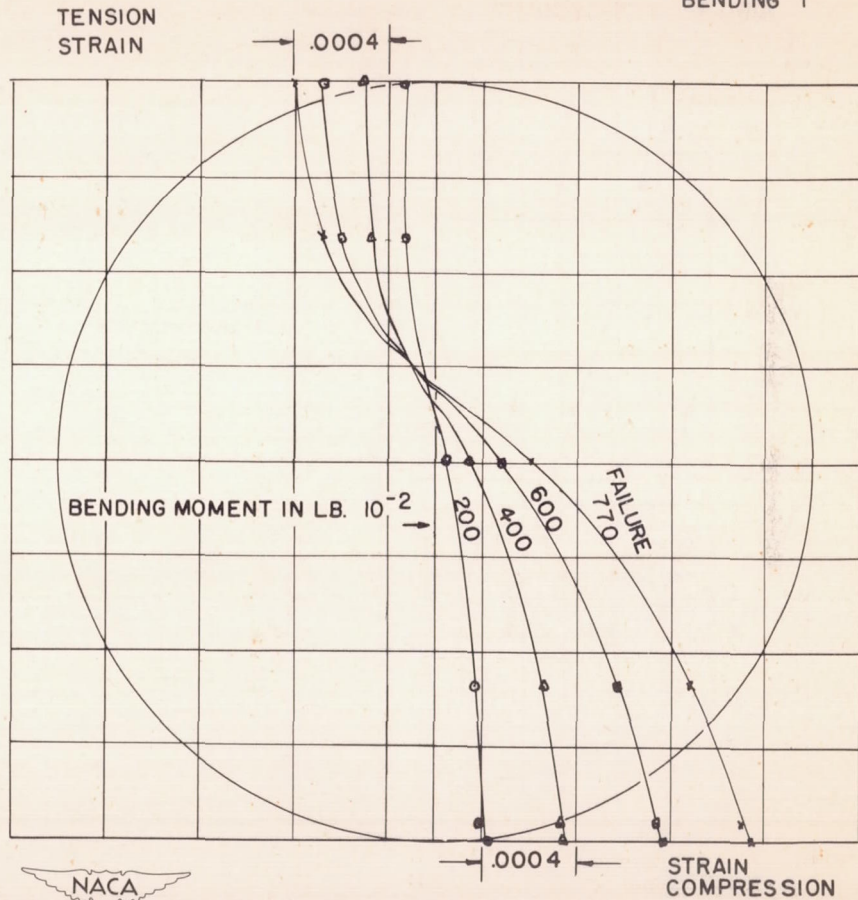


FIGURE 9.

SPECIMEN 152
 TORSION $\frac{2}{1}$
 BENDING $\frac{1}{1}$

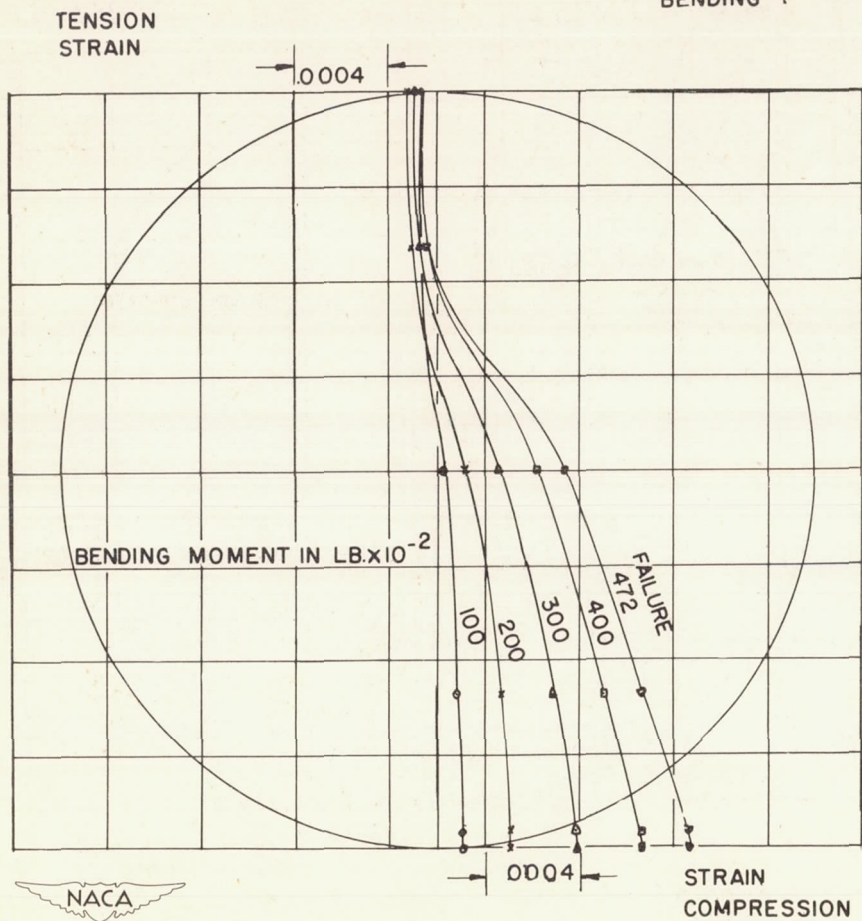


FIGURE 10.

SPECIMEN NO. 150
 TORSION $\frac{5}{1}$
 BENDING $\frac{1}{1}$

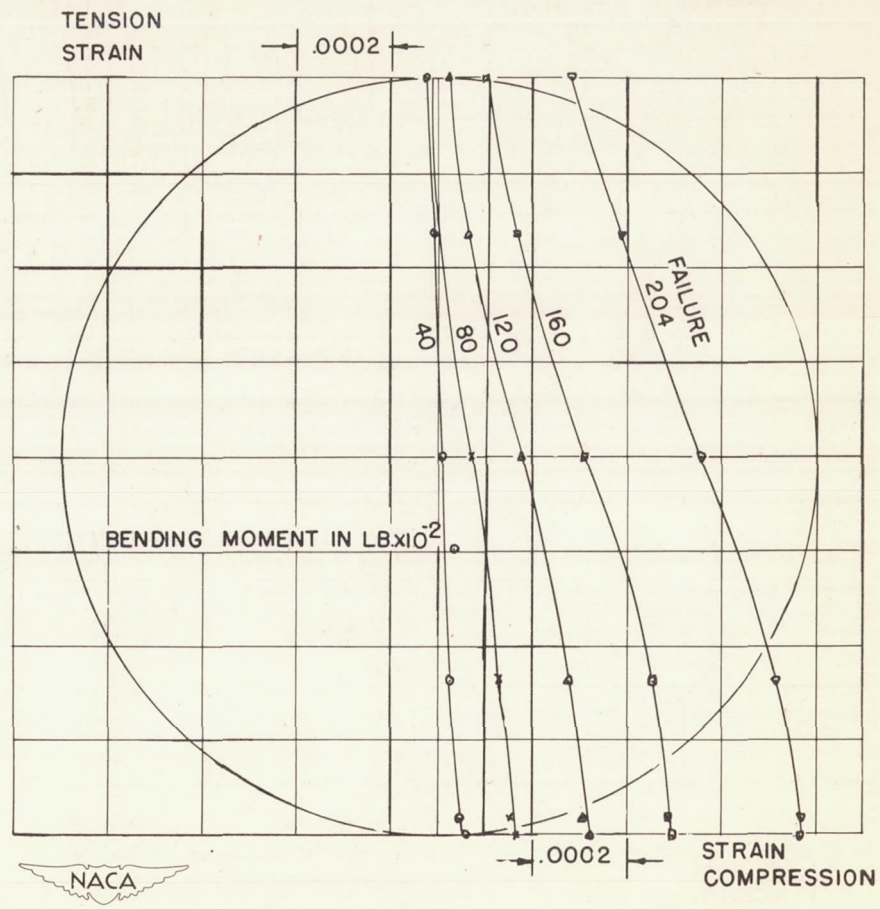


FIGURE 11.

SPECIMEN NO. 149
PURE TORSION

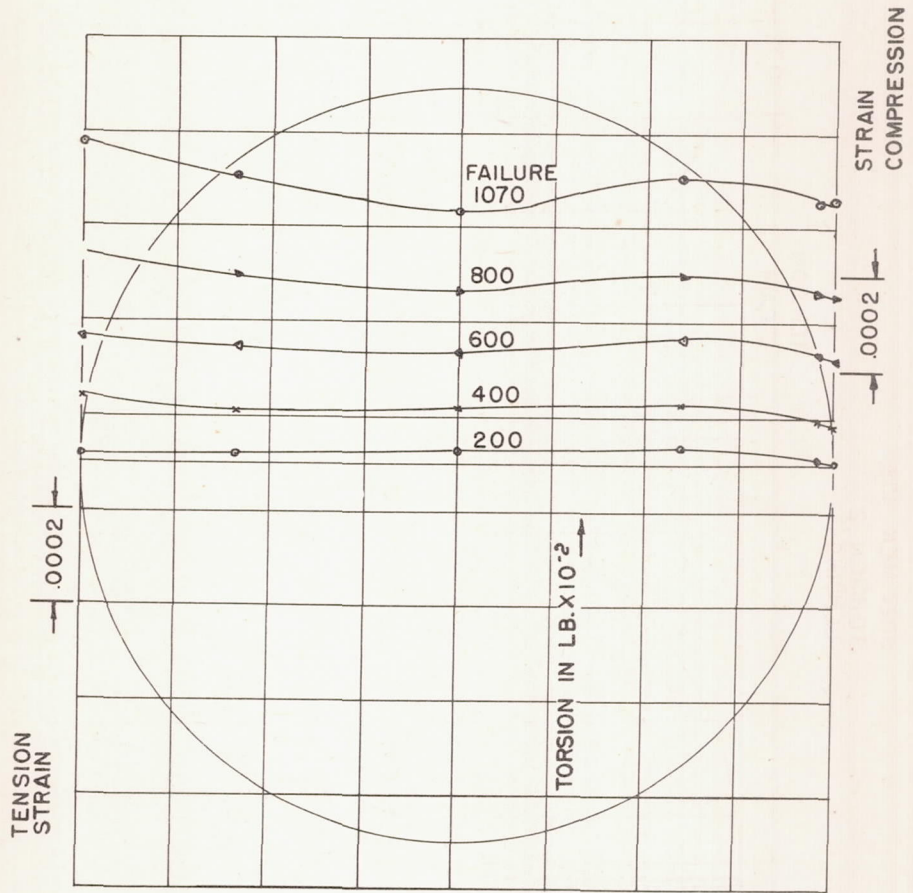


FIGURE 12.

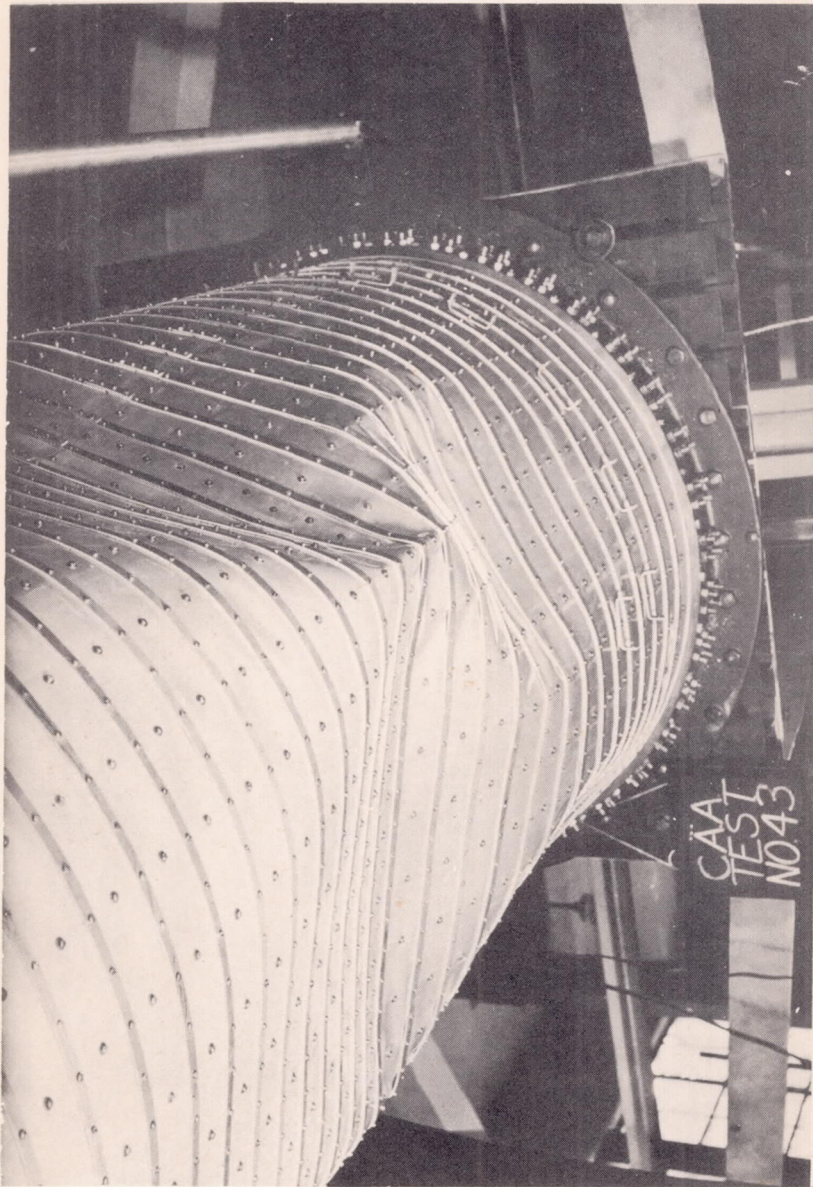


Figure 13.- Pure bending failure.



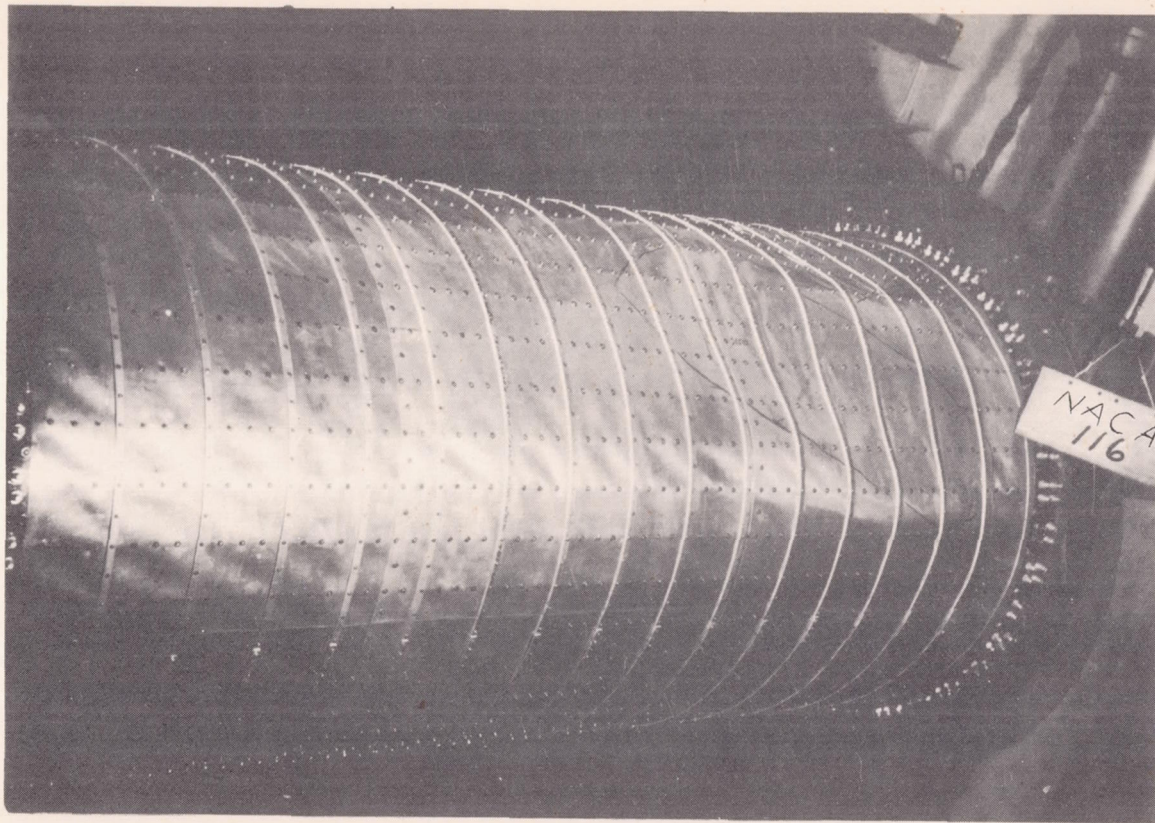


Figure 14.- Combined bending and transverse shear. Failure occurred in maximum compression zone.



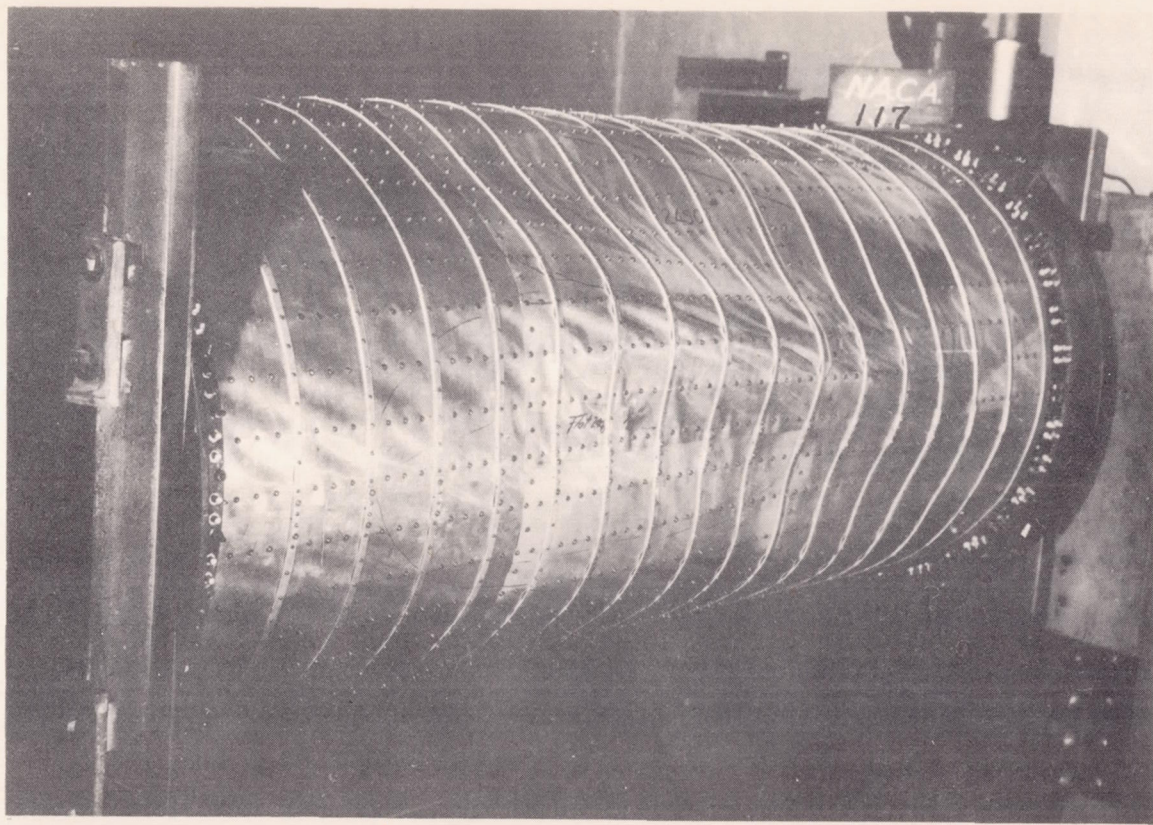
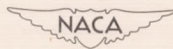


Figure 15.- Combined bending and transverse shear. Failure occurred in maximum shear zone.



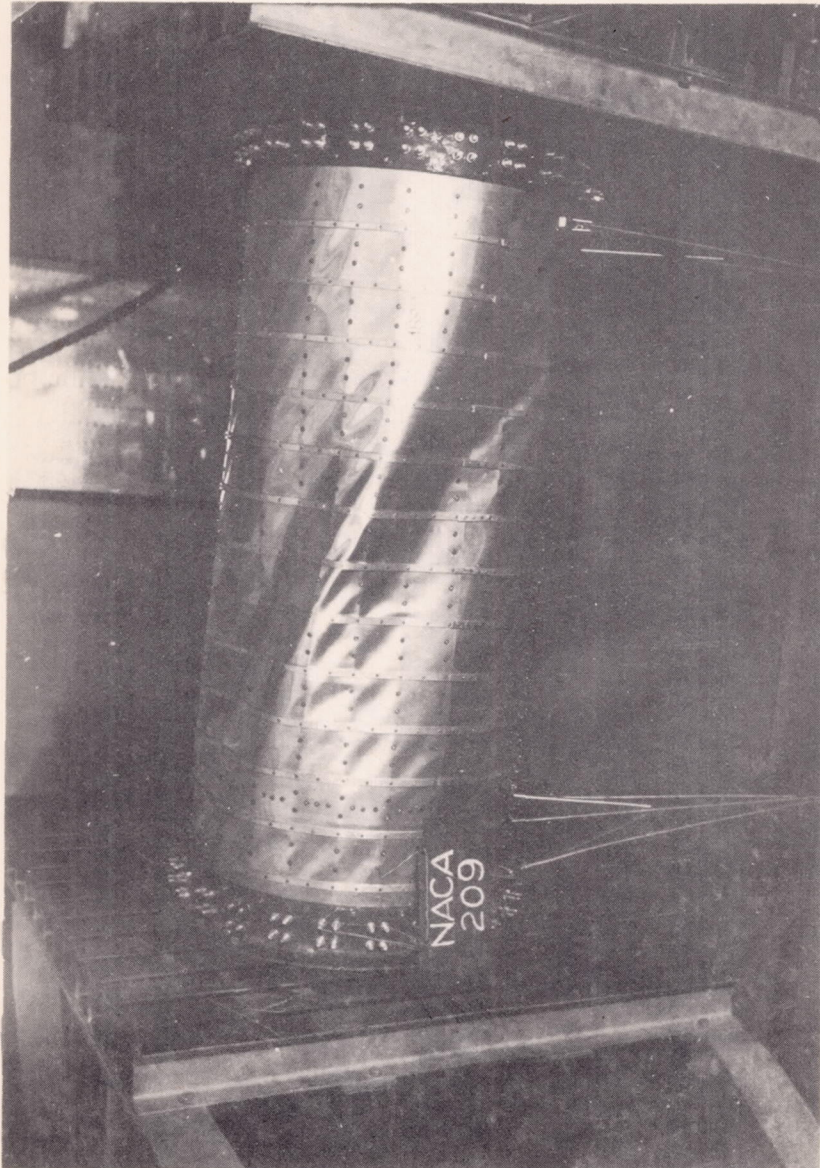


Figure 16.- Pure torsion failure.



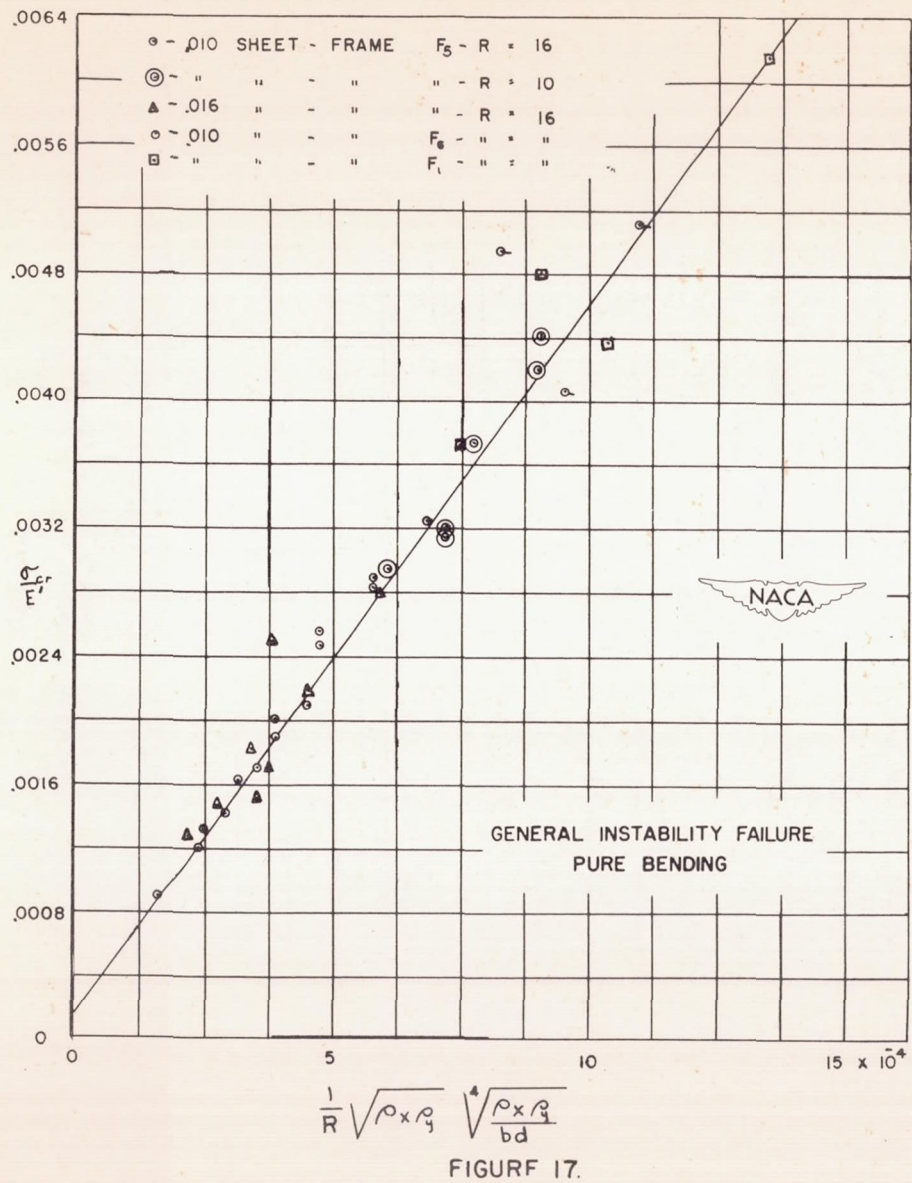


FIGURE 17.

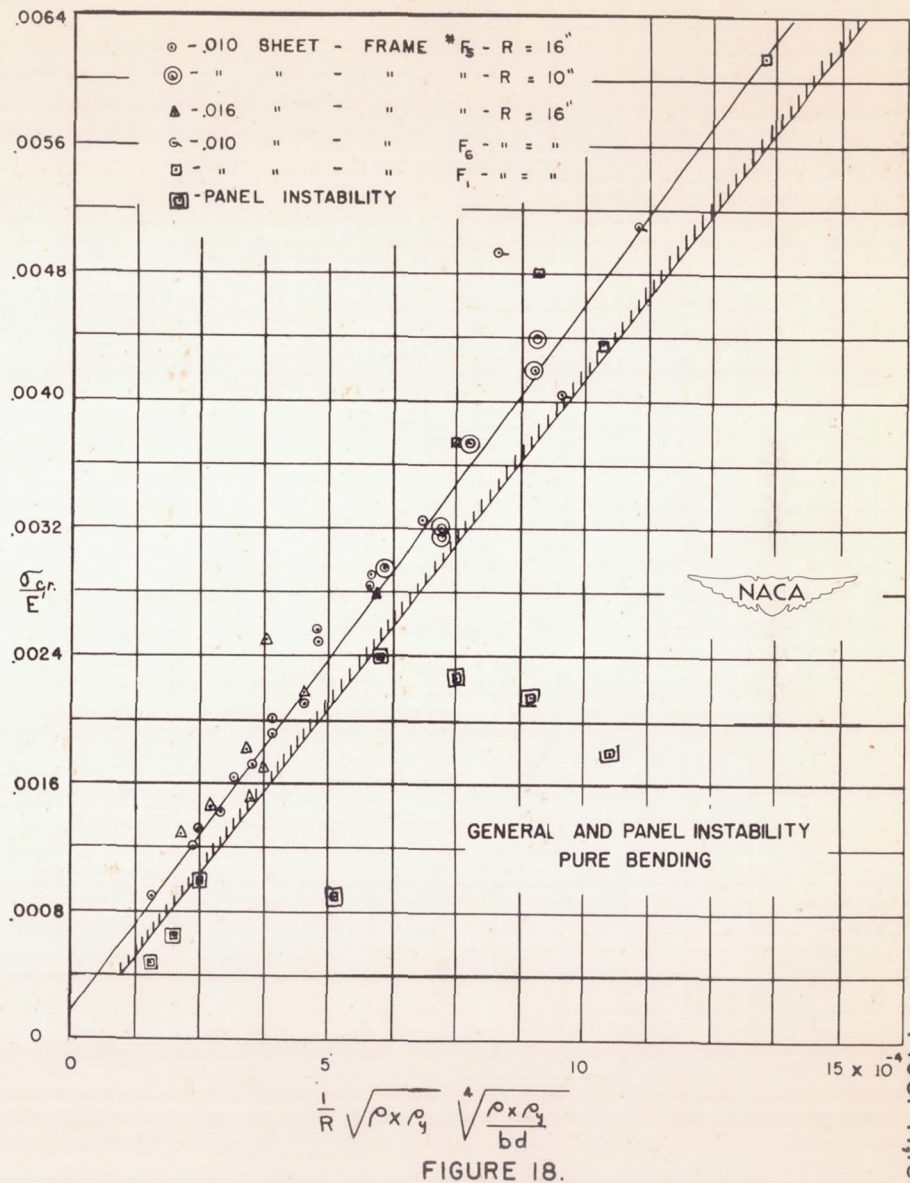


FIGURE 18.

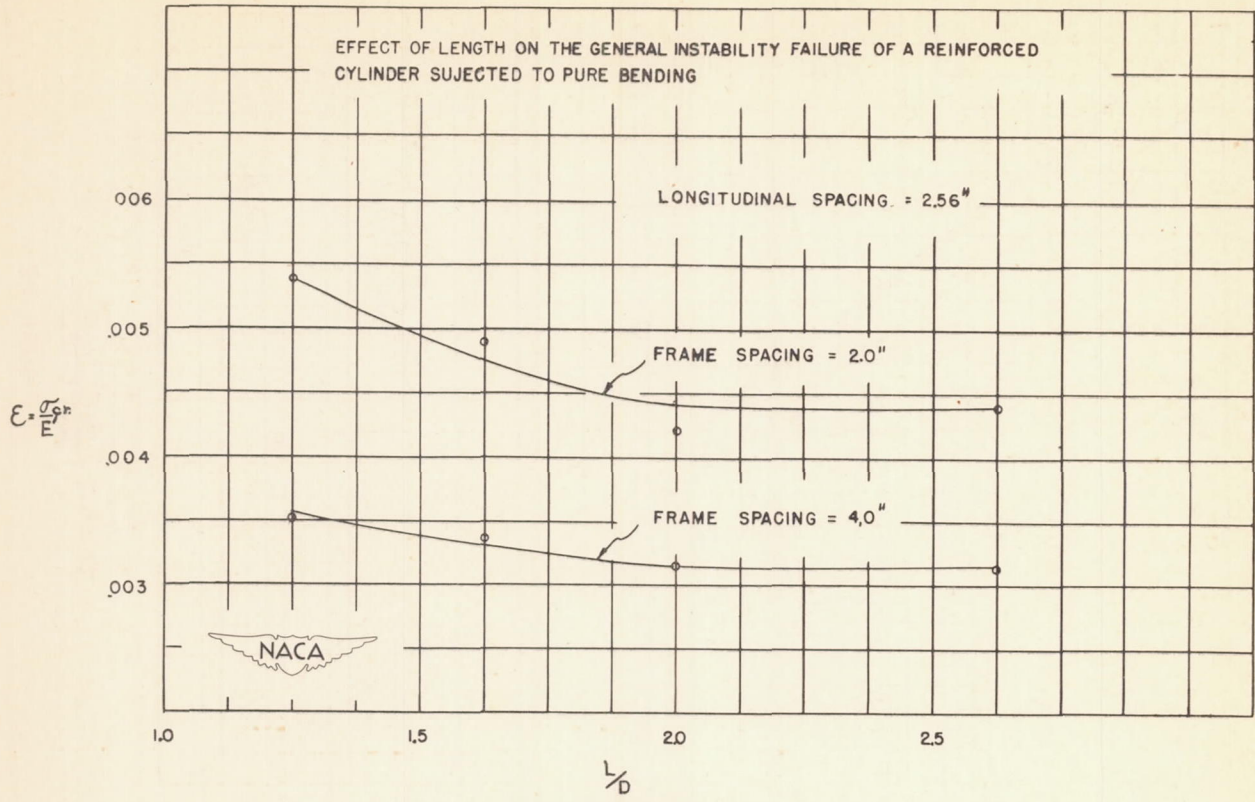


FIGURE 19.

○ 75 - 78 & 92
 □ 118 - 121

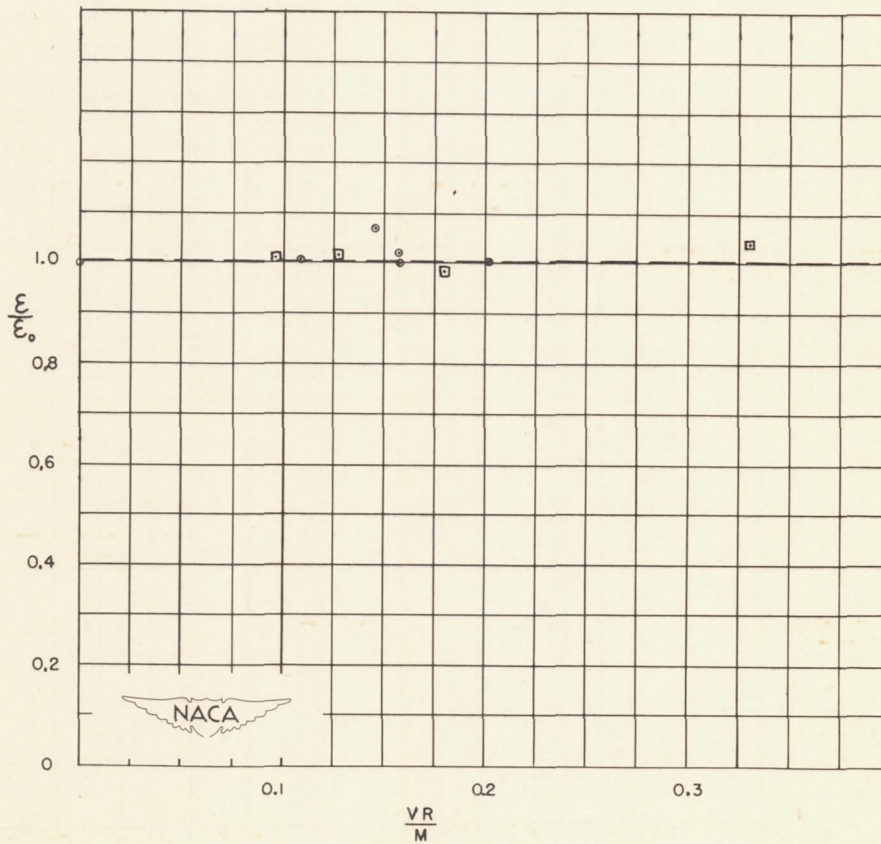


FIGURE 20.

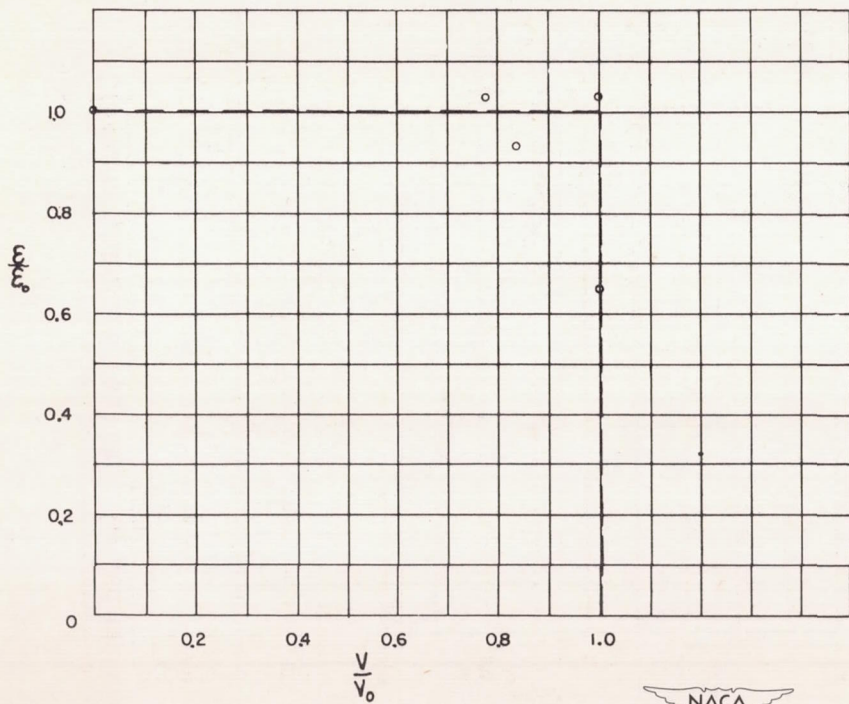


FIGURE 21.

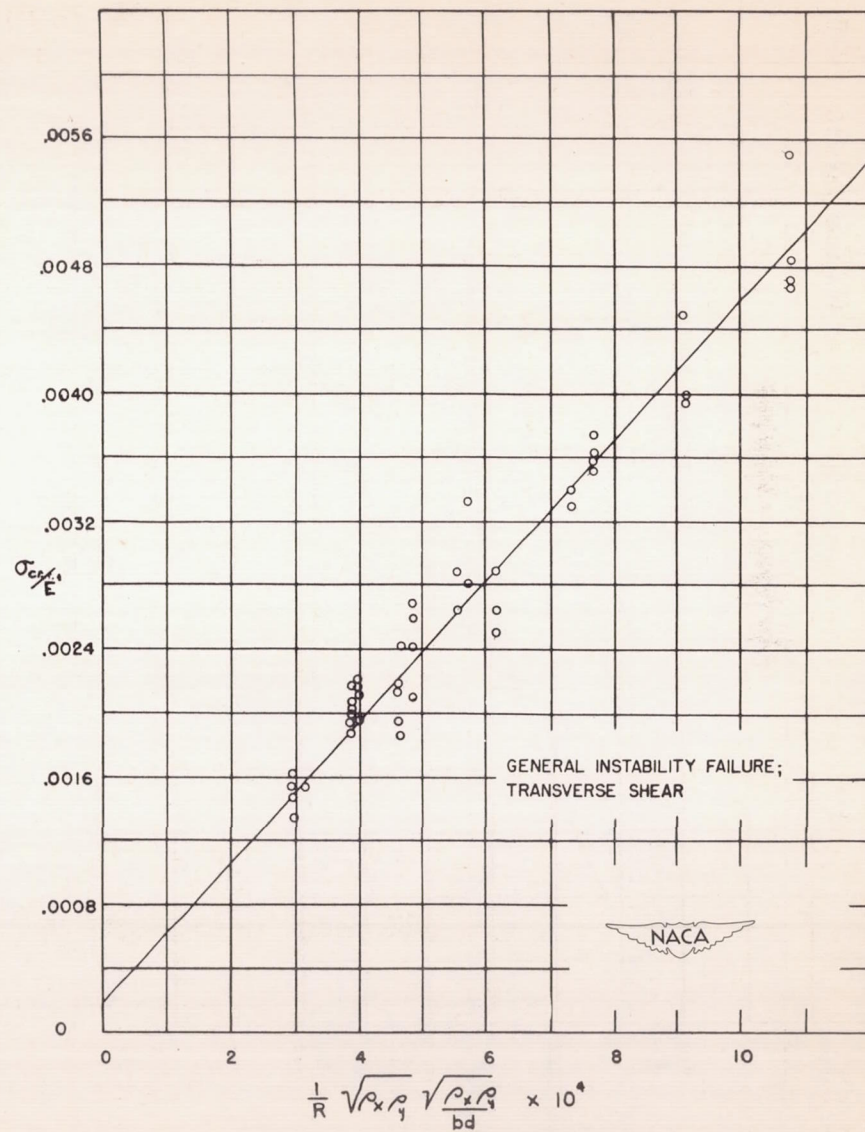


FIGURE 22.

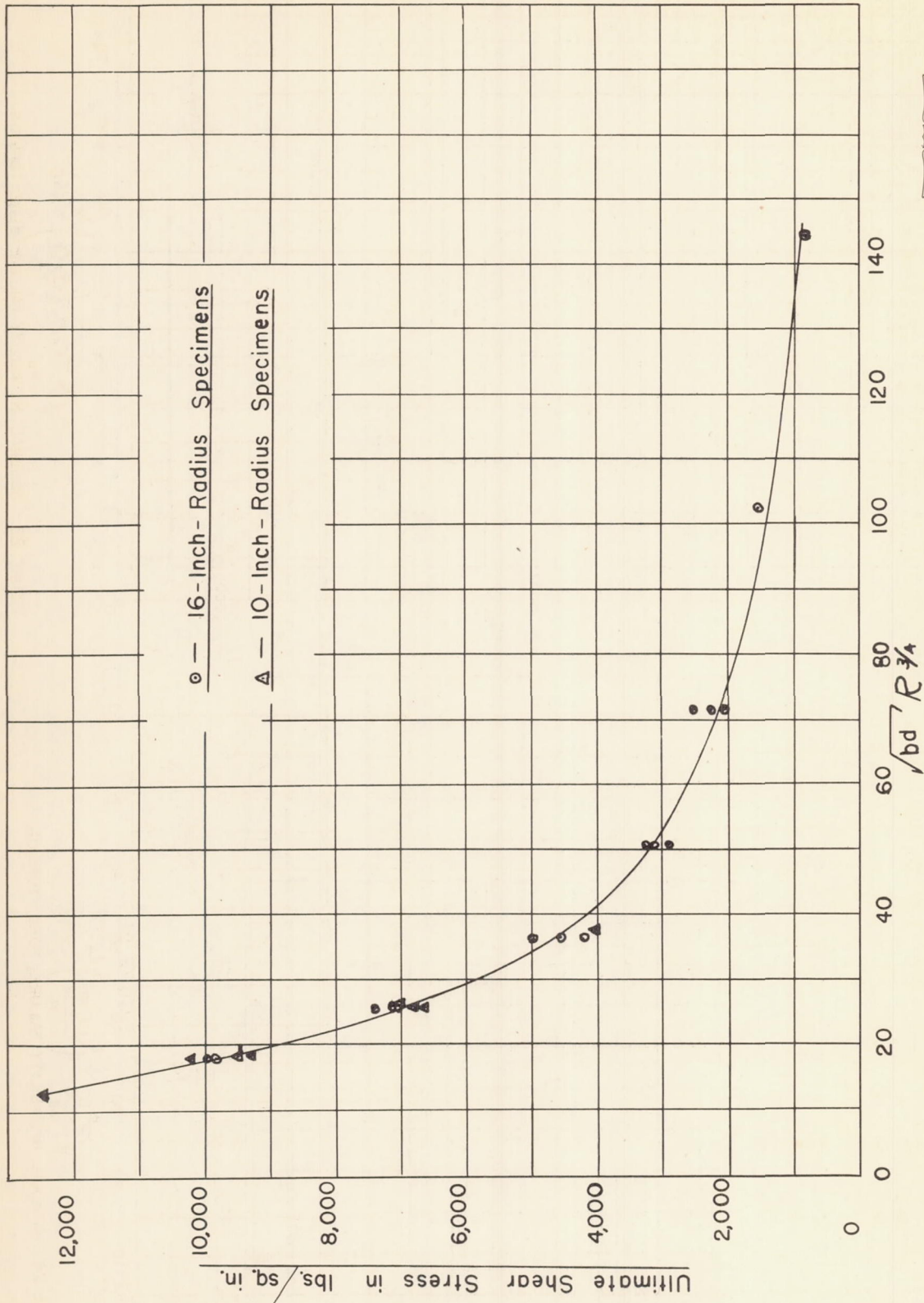


FIGURE 23.

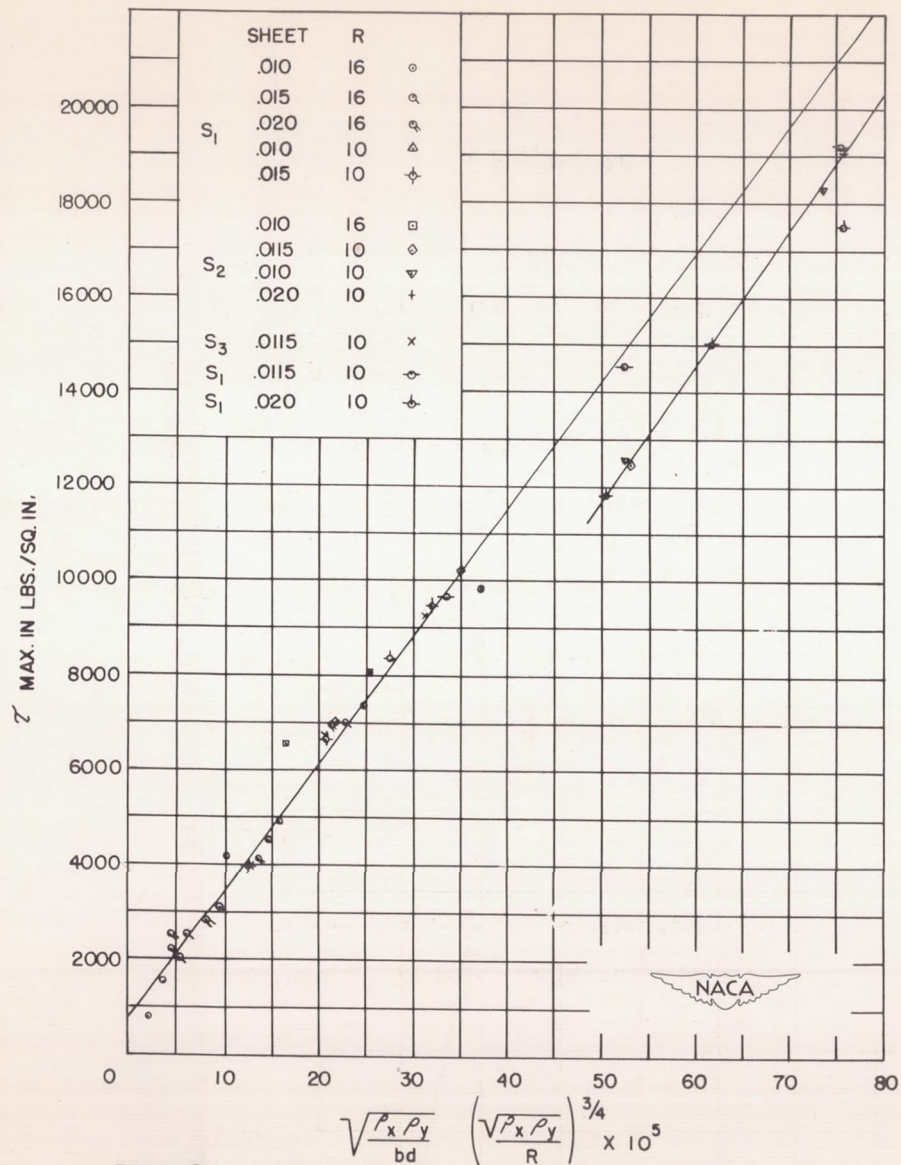


FIGURE 24.- GENERAL INSTABILITY FAILURE; PURE TORSION.

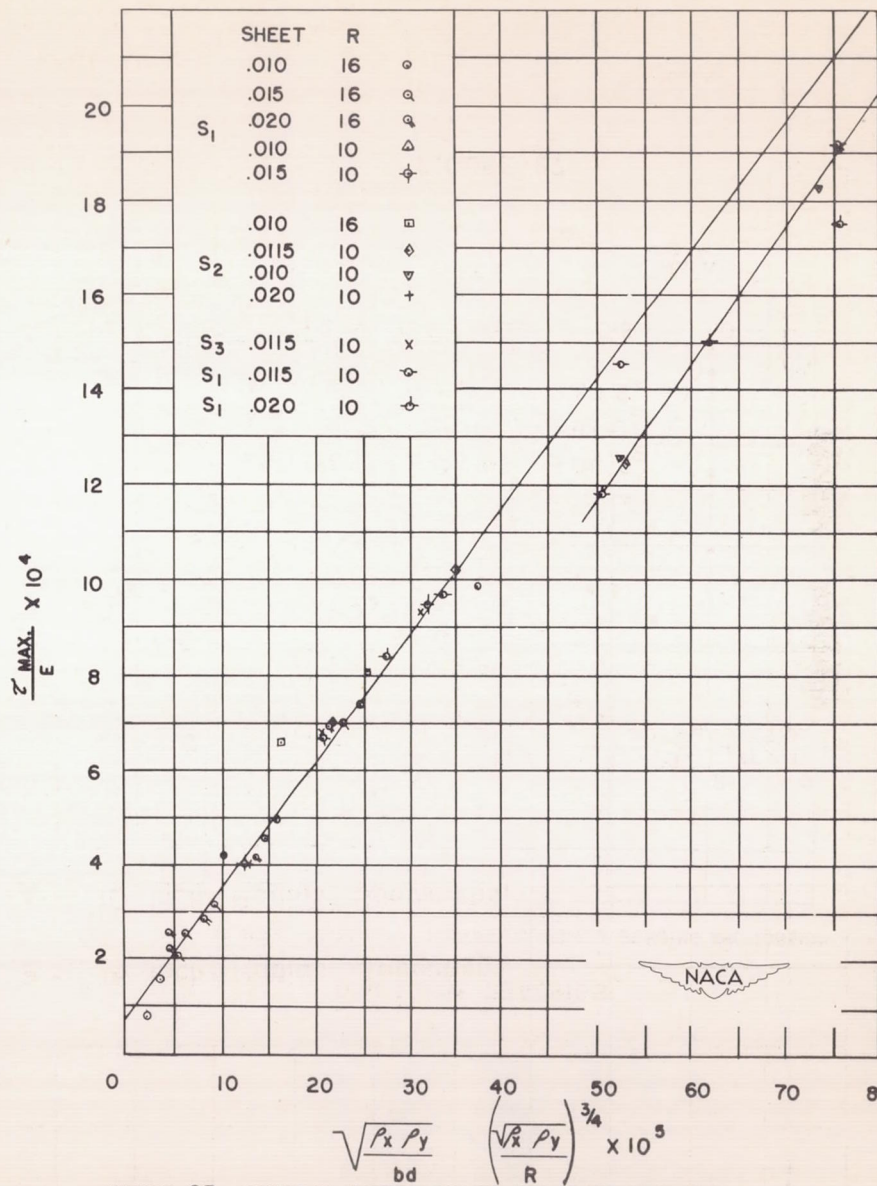


FIGURE 25.- GENERAL INSTABILITY FAILURE; PURE TORSION.

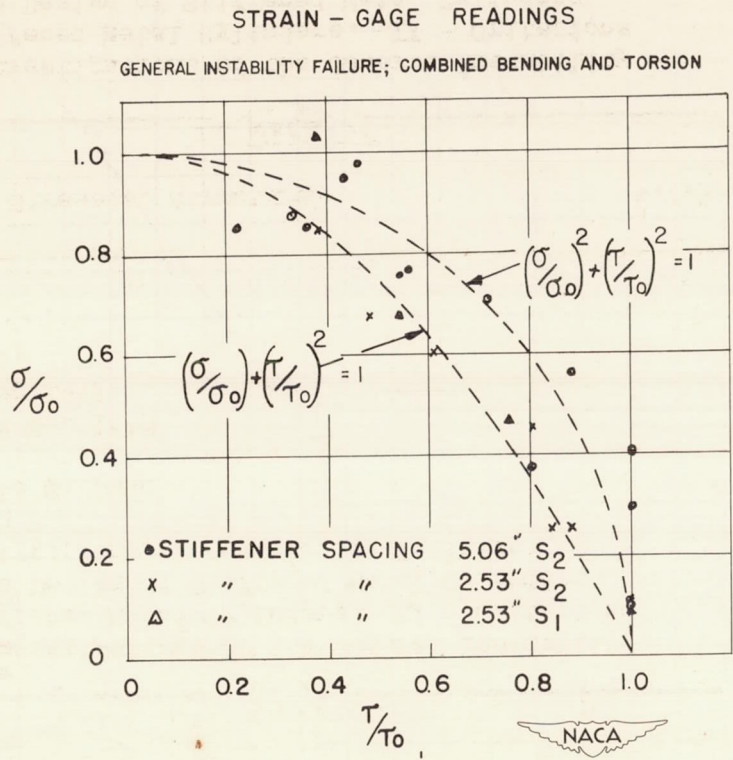


FIGURE 26.

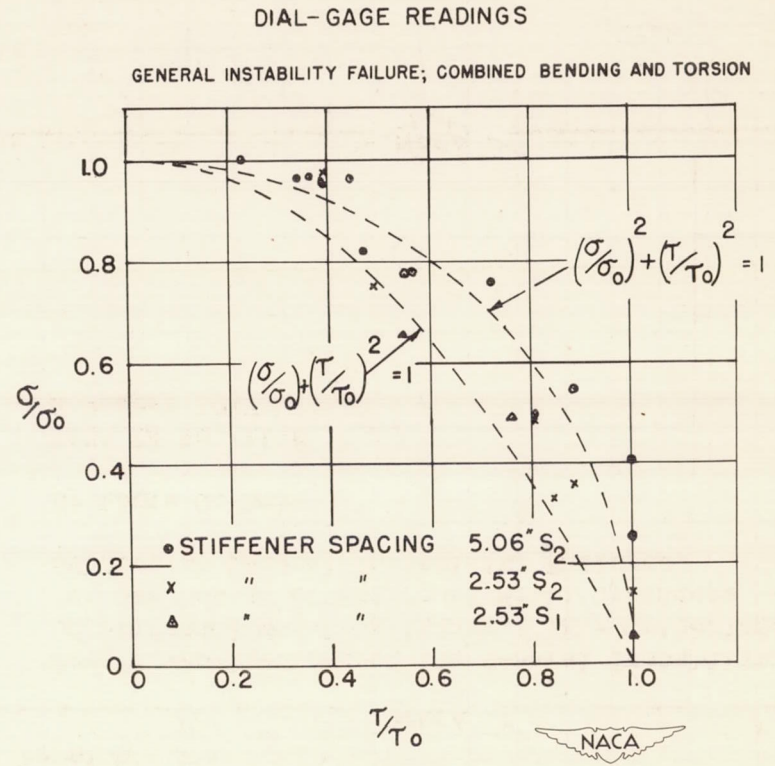


FIGURE 27.